Materials Advances

ROYAL SOCIETY OF CHEMISTRY

REVIEW

View Article Online
View Journal | View Issue

Cite this: *Mater. Adv.*, 2025, 6, 8337

An overview of porphyrin-comprising supramolecular scaffolds for cancer phototherapy

Fatemeh Ganjali, Saminalsadat Sehat, Sepide Azadegan, Maryam Saidi Mehrabad, Leila Choopani and Ali Maleki *

Photothermal and photodynamic treatments, as the primary branches of phototherapy, are derived from non-invasive therapies. Since metal–organic frameworks (MOFs) and covalent–organic frameworks (COFs) are advanced crystalline and highly porous materials, they have attracted considerable attention and played a significant role in phototherapy due to their innate porous structure, flexible design, regularity in structure, multifunctionality, and favorable biocompatibility. Porphyrin and its derivatives have emerged with outstanding electrochemical and photophysical characteristics, which have garnered remarkable attention in various fields, including catalysis, biosensing, solar cells, biomedical applications, and gas storage. Nonetheless, porphyrin's applicability in cancer phototherapy is limited due to its intrinsic limitations, such as weak absorption in the biological spectral window, poor optical and chemical stability, and self-quenching. Porphyrin-comprising MOFs and COFs, a group of new hybrid porous coordination polymers, are introduced to overcome the porphyrin's restrictions and develop its biomedical applicability. Encapsulating porphyrins into the pores of these supramolecular scaffolds, grafting porphyrins onto their surface, or utilizing porphyrins as structural organic linkers enables the combination of the particular characteristics of these supramolecular scaffolds and porphyrins, thereby overcoming the limitations of porphyrins in biomedical applications. This review provides a historical overview of cancer phototherapy, including a brief outline, synthesis routes, and the applications of porphyrin-comprising MOFs and COFs in phototherapy. Ultimately, the challenges and outlook on cancer phototherapy using these substances are debated.

Received 23rd May 2025,
Accepted 4th August 2025

DOI: 10.1039/d5ma00531k

rsc.li/materials-advances

1. Introduction

One of the most prominent causes of death is cancer, which has become a global issue. In recent years, several million cancer-related deaths have been reported in the world. Cancer happens when cells grow abnormally and can occur in different organs of the human body, such as the breast, gastrointestinal tract, skin, *etc.* Current cancer treatments are based on chemotherapy, surgery, radiotherapy, immunotherapy, and phototherapy.[1] Chemotherapy uses anti-cancer drugs, such as doxorubicin (DOX),[2] paclitaxel,[3] *etc.*, which lead to side effects because they also damage normal cells. Recently, nanotechnology has enabled the development of therapeutic methods to maximize the benefits of each approach and reduce side effects. Some anticancer drugs induce apoptosis by damaging the DNA within the cell. Drugs such as DOX and cisplatin use this mechanism to treat cancer, allowing them to be rapidly distributed throughout tissues and kill cancer cells when they come into contact with them. However, these drugs have side effects due to their high toxicity. One of the side effects observed as a result of treatment with cisplatin is kidney damage, which is observed due to the production of excessive free radicals. In this regard, alternative methods for direct drug entry and distribution throughout the human body have been developed.[4]

Among the various treatment methods, phototherapy has been highlighted because near-infrared (NIR) light penetrates the skin and has two mechanisms: photodynamic therapy (PDT) and photothermal therapy (PTT), which can induce apoptosis and necrosis in cancer cells.[5] Combining phototherapy and nanotechnology in medicine has promoted and developed the usage of visible light in various skin diseases and cancers. It can be a method with fewer side effects and less invasive than other methods. Organic or inorganic materials that can increase the efficacy of PTT and PDT are essential in this context. Therefore, different inorganic sensitizing structures with heat-generating capacity, such as gold nanoflowers,[6] iron nanoparticles (NPs),[7] copper NPs,[8] gold/silver NPs,[9] *etc.*, have been examined. PTT can fight disease by generating heat in the environment and causing cell apoptosis. In addition, the

Catalysts and Organic Synthesis Research, Laboratory, Department of Chemistry, Iran University of Science and Technology, Tehran, Iran. E-mail: maleki@iust.ac.ir; Fax: +98-21-73021584; Tel: +98-21-73228313

existence of effective structures for producing reactive oxygen species (ROS) in cells could significantly enhance cancer cell death and PDT performance, as this method relies on the creation of free radicals that damage the membrane, ultimately destroying the cancer cells.[10] Organic photosensitizers (PS) structures can be a suitable alternative for improved performance in the body, offering more outstanding biocompatibility and the production of ROS. Consequently, selecting the type of PS is crucial, as it should possess stable chemical properties and exhibit low toxicity to the body. The ideal PSs are porphyrins and their diverse derivatives with a facile synthesis route. These structures function well in the body, allowing them to be effective in PTT and PDT by producing ROS with thermal stability. They cause less damage to normal tissues and lead to cancer cell death. Based on its unique physicochemical features, porphyrin is used in drug delivery systems, diagnosis, and imaging.[11,12]

One of the challenges is the internalization of porphyrin and selecting a carrier type that can enter the cancer cell. Various types of carriers have been reported in recent years due to the widespread utilization of porphyrin in drug delivery and phototherapy. Bera *et al.* introduced a multifunctional carrier by loading DOX into a porphyrin structure conjugated with gold NPs to induce the apoptosis of cancer cells using the PDT

Fatemeh Ganjali

Fatemeh Ganjali, born in Isfahan in 1994, is a distinguished researcher in the field of nanotechnology. She earned her BSc in Applied Chemistry from the Islamic Azad University of Shahreza (IAUSH) in 2018, followed by an MSc in Nanochemistry from Iran University of Science and Technology (IUST) in 2020, where she graduated as the top student. Currently pursuing her PhD in nanotechnology (nanopolymer) under the supervision of Prof. Ali Maleki at IUST, her research focuses on nano-biotechnology, with particular interests in hyperthermia, magnetic nanocomposites, and advanced polymeric systems. Her scholarly contributions include several ISI articles and ten chapters in a published volume on metal–organic frameworks (MOFs) and their multifaceted applications in nanomaterials science. Her work exemplifies a rigorous commitment to innovation at the intersection of chemistry and materials science.

Saminalsadat Sehat

Saminalsadat Sehat was born in Tehran in 1995. She received her BSc in Chemistry of Information Technology from the Islamic Azad University, North Tehran Branch, in 2019. She completed her MSc in Nanochemistry in 2022 at Iran University of Science and Technology (IUST) under the supervision of Prof. Ali Maleki. In 2023, she began her PhD studies in Nanochemistry at IUST with a high GPA. Her research focuses on nano-biotechnology, particularly targeted drug delivery systems and tissue engineering, to develop more effective and precise therapeutic strategies. Her work has potential applications in cancer treatment and regenerative medicine. She has published several articles in high-impact journals and contributed to a book chapter. She is committed to advancing the field of Nanochemistry and aims to design innovative nanocarriers for precision medicine and biomedical applications.

Sepide Azadegan

Sepide Azadegan was born in Tehran in 1986. She received her Master's degree in nanochemistry from the Iran University of Science and Technology. Her enduring passion for research has led to the publication of four ISI articles. Sepide has an impressive background in the pharmaceutical industry, having attended several pharma-related workshops and worked for renowned companies in the field. Recently, she achieved a 6.5 score in the Academic IELTS and is continuously learning German to reach the B1 level. Notably, she has maintained her connection with the academic and research community post-graduation, continuing her work in bio-related nanomaterials.

Maryam Saidi Mehrabad

Maryam Saidi Mehrabad was born in Tabriz in 1994. She holds a MSc in Nanochemistry from Iran University of Science and Technology and a BSc in Applied Chemistry from Tabriz University. She has published peer-reviewed research in leading outlets, including the ACS and Springer. Her works include the journal article "Effective Combination of rGO and CuO Nanomaterials through Poly(p-phenylene diamine) Texture: Utilizing It as an Excellent Supercapacitor" and the book chapter "Evolution in MOF Porosity, Modularity, and Topology". Her research focuses on nanomaterials, supercapacitors, and metal-organic frameworks.

method, as well as for drug delivery and dose control.[13] A porphyrin-containing liposomal drug delivery carrier for cancer cells was introduced by Wang *et al.*, who showed that the anticancer drug loaded in this nanocarrier successfully induced DNA damage in the cancer cells' nucleus.[14] When light shines on a material, it can transfer its energy to the electrons in the material. This causes the electrons to jump to a higher energy level, leaving a hole (an electron vacancy) in the lower level. This pair is known as an electron/hole (e/h) pair. In nanoscale materials, the distance that this electron and hole must travel to reach the surface (or recombine) is much shorter than that in conventional, bulk materials. The shorter path reduces the likelihood of rapid recombination. It increases the lifetime of electron–hole pairs, enabling their use in processes such as electric current generation, light emission, and chemical reactions. For example, for optimal use, a composite such as a MOF–metal oxide composite can be used, which will result in maintaining stability at a lower cost.[15] In the case of the porphyrin and its derivatives, NIR light irradiation causes the production of ROS and the release of CO_2, ultimately accelerating the apoptosis process. Therefore, MOFs, with their high storage capacity and surface area, facilitate the production of ROS.[16]

Covalent and non-covalent scaffolds can be used as carriers in drug delivery,[17,18] phototherapy,[19,20] imaging, and diagnosis.[21,22] Because of high porosity with synthetic tunability, facile synthetic route, surface absorption, ion exchange, and large surface area, these structures can accommodate drugs and PSs.[18] By creating coordination bonds, metal–organic frameworks (MOFs), possessing metal ions and organic ligands, could contain PSs like porphyrin and its derivatives in their structure. These coordination polymers can encapsulate other molecules or structures, such as drugs, enzymes, or precious metals, within their cavities or retain them in the environment through their host–guest action and high chemical stability. These molecules can sometimes be part of the framework itself and can be used as ligands. In various cases, this has also been seen for anticancer drugs to reduce their toxic effects and act specifically. The possibility of using different structures and combining them with various metal nodes, creating highly porous and diverse structures with holes, is one of the features that makes these frameworks special. With MOF-based carriers, several therapeutic methods, such as chemotherapy, can be combined with sonodynamic therapy (SDT), PTT, or PDT. By creating a synergistic effect, the mortality rate of cancer cells can be increased.[23] Porphyrins serve as either structural linkers during the formation of these porous materials or as guest molecules occupying their internal cavities.[24,25] Yaghi *et al.* introduced the first synthesized MOF, and the synthesis of porphyrin-based MOF was presented in 1991.[26–28]

Another class of polymer frameworks are found at the nanoscale, which have created unique physicochemical properties through the formation of covalent bonds. These frameworks are trending because they exhibit low density, biocompatibility, thermal stability, and high loading capacity. These structures, called covalent–organic frameworks (COF), can contain porphyrin compounds and ultimately lead to the high stability of porphyrin in the human body and solve the problem of poor solubility of porphyrin, thus showing good performance in drug delivery and phototherapy.[29,30] It is worth emphasizing that the first paper on COFs by condensation reactions was published by Cote and Yaghi *et al.* in 2005.[31] Hu *et al.* prepared a porphyrin-based COF-366 nanoplatform with pH-responsiveness, which inhibited liver carcinoma with drug release and PDT.[32] The COFs are very strong with covalent bonding and can be used in various applications using porphyrin ligands to create adjustable cavities. With this feature, molecules or structures of specific size can be inserted into the cavities inside the COF, leading to host–guest chemistry.[33] In general, in host–guest chemistry, supramolecular frameworks are used to create physical interactions and porous spaces, which is one of their applications in cancer treatment using PSs as guests. For example, Wang *et al.*

Leila Choopani

Leila Choopani, born in Tehran, holds a Bachelor's in Chemistry from Imam Khomeini International University and a Master's in Organic Chemistry from Iran University of Science and Technology (IUST), where she graduated in 2022. Her research focuses on environmental restoration, sustainable chemistry, eco-friendly materials, and biotechnology. Actively involved in various projects, Leila aims to address environmental challenges and promote sustainability. Committed to expanding her knowledge, she seeks to contribute innovative solutions that help create a cleaner planet. She aspires to make a meaningful impact in chemistry and environmental science through collaboration with other researchers and professionals.

Ali Maleki

Prof. Dr Ali Maleki was born in Mianeh, East Azerbaijan, in 1980. He received his PhD in Chemistry in 2009. He started his career as an Assistant Professor at the Iran University of Science and Technology (IUST) in 2010, where he is currently a Full Professor. His research interests focus on the design and development of novel catalysts, nanomaterials, and green chemistry. He has hundreds of ISI-JCR publications. Some of his honors include being named the Distinguished Researcher of IUST from 2010 to 2023, the IUPAC Prize for Green Chemistry in 2016, and being recognized as one of the Top 1% International Scientists in ESI (Web of Science) from 2018 to 2025.

modified genes using a type of PS that is incorporated as a guest in the MOF to enhance its PDT effect along with gene therapy in cancer cells.[34] Of course, host–guest structures using porphyrin-based MOFs (PMOFs) are also utilized in other industries.[35]

In line with the PDT enhancement, significant advances have been made in preparing photosensitizers, particularly those comprising porphyrins.[36] According to previous studies, many photosensitizers used in cancer treatment consist of a porphyrin-containing macrocyclic skeleton.[37,38] For instance, hematoporphyrin derivative has shown an outstanding therapeutic impact when exposed to light irradiation.[39] However, sodium porphyrin is the first authenticated photosensitizer in cancer treatment.[36] Although porphyrin is extensively used in PDT due to its photosensitive characteristics, it has downsides in cancer therapy, which are reported in the previous literature.[40] Porphyrins have high extinction coefficients and singlet oxygen quantum yields. In addition, porphyrins are stable in the ultraviolet to infrared region and can absorb light in the therapeutic wavelength region, and can induce photodynamic therapy effects. Porphyrins have low solubility and lack targeting ability on their own. This shortcoming should be considered when using porphyrin photosensitizers to enhance the effectiveness of light energy absorption and therapy. Previous studies have reported the mechanism of PDT and discussed NPs.[41–43] This review not only focuses on the porphyrin photosensitizer but also highlights the improvement of its characteristics after incorporating it into MOFs and COFs, demonstrating its synergistic impact in phototherapy and indicating the overcoming of the bare porphyrin's downsides in biomedical applications.

While previous reviews focused only on PMOFs[44,45] or just on porphyrin-based COFs (PCOFs)[46,47] for cancer phototherapy, this work emphasizes both MOFs and COFs containing porphyrin, whether it is encapsulated in the MOFs' pores or grafted on the surface, or as an organic linker to form porphyrin–MOFs. In this review, along with the study of the phototherapy method, a particular species of PS has been discussed, which can enable cancer treatment using supramolecular frameworks, as well as the latest articles that have investigated the preparation methods, their benefits, and performance in the treatment of cancer in recent years have been reviewed with a comparative perspective.

2. A historical survey of cancer phototherapy

Cancer has spread as a devastating, fatal disease. It has been significantly observed that applying traditional treatments such as radiotherapy, chemotherapy, and surgery has increased the destruction of cancerous tumors. Adverse consequences of clinical therapies have been demonstrated in these investigations. Moreover, there are significant challenges with medication cytotoxicities and resistance. Researchers are creating reliable, affordable, and secure alternatives to address this issue.[48,49] The general definition of phototherapy is the application of photons to medical conditions without needing an external PS. Standard blue, daylight, and cool white lamps used in fluorescent tubes are considered classic phototherapy equipment. Thanks to technology, three primary modalities of phototherapy administration are currently available to clinicians: fiber optic, low-intensity, and high-intensity phototherapy.[50]

PTT and PDT frequently employ phototherapy, which involves the application of light radiation to tissues. Both methods are non-invasive treatments with extremely effective therapeutic effects. To discuss the reasons for applying PSs, the following factors are considered most important: increasing photothermal reactions in PTT and singlet oxygen ($^1O_2$) generation in PDT, as well as enhancing the selectivity and efficacy of phototherapy. As a cancer therapeutic approach, PDT has drawn increased attention lately. It is a targeted and selective method that improves specificity against cancer cells. To study in-depth, PDT uses PSs and light to produce ROS, which kill malignant cells. The choice of PSs, however, is crucial to the effectiveness of PDT, as the given PS must penetrate deeply into the tumor cells before being activated by light radiation. PDT causes cell death, which is the result of the apoptotic reaction of PS's subcellular localization. Under light irradiation, PSs absorb photons to form charge carriers. Afterwards, excited singlet electrons undergo intersystem crossing to form long-lived excited triplets; they undergo relaxation, transforming their energy into heat, fluorescence, and/or other photophysical energy forms. The excited electrons are unable to return to the ground state (GS) due to collisions or aggregation between molecules, and some of the energy will be dissipated as heat.[50,51]

In contrast to PTT, PDT uses the generation of ROS and the conversion of electron energy to oxygen to destroy tumor cells. The amount of ROS produced in the cells during PDT directly impacts the therapeutic outcome. On the other hand, a hypoxic environment and high glutathione levels at the tumor site significantly reduce ROS production.[52] To induce apoptosis or necrosis through the action of $^1O_2$ and other ROS, PDT relies on the selective retention of PSs in tumor tissue and the presence of O_2 after irradiation at an appropriate wavelength.[53] A particular excitation light, $^1O_2$, and PS are all part of PDT.

After being injected into the patient's body, the PS concentrates in tumor tissue selectively, causing the lesion to be illuminated with light of appropriate energy wavelength. After that, the PS absorbs energy to undergo an energy level transfer, sending the molecule from its GS to an impermanent singlet excited state (^{1}ES). Afterward, it undergoes an intersystem transmission to the triplet excited state (^{3}ES). Ultimately, through various photochemical reactions, such as types I, II, and III, the tumor cells will be eradicated. The following is a brief description of their processes: Type I, when the PS molecule enters a ^{3}ES, it combines with O_2 to produce free radicals of oxygen, including hydroxyl ($^{\bullet}OH$) and superoxide ($O_2^{\bullet-}$) radicals. To generate sufficient superoxide radicals, the photogenerated electrons can efficiently reduce the dissolved oxygen; Type II through the use of PSs, GS oxygen is excited into $^1O_2$ by transferring the absorbed energy to the nearby oxygen molecules; and Type III (the PS molecule in the ^{3}ES kills tumor cells by damaging their DNA directly when oxygen is not present) (Fig. 1(a)). The most widely

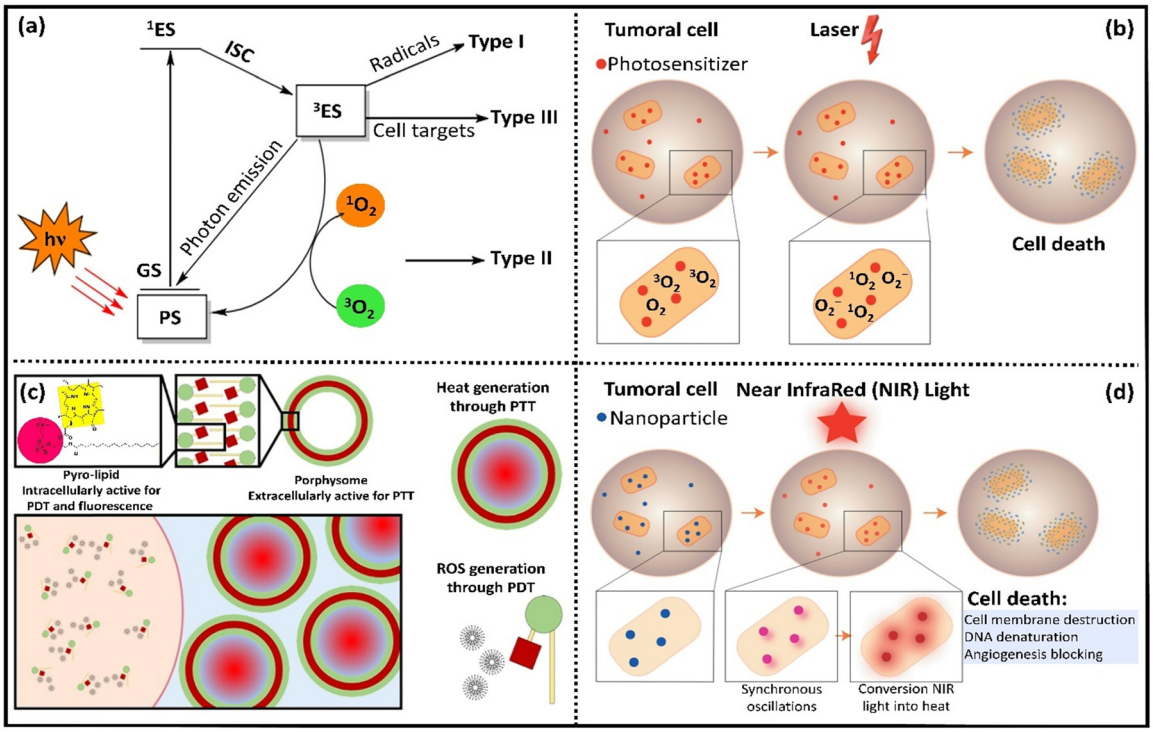

Fig. 1 (a) Graphical explanation of the PDT mechanism based on the energy diagram of Perrin–Jablonski. This figure was reproduced from *ChemMedChem*, 2020, **15**, 1766–1775.[55] (b) PS and ROS contribute to cell death during the PDT procedure, as well as in immunological responses against tumors. This figure was reproduced from *Pleura Peritoneum*, 2018, 20180124.[56] (c) Diagram showing how porphysome NPs and dissociated pyro-lipids are distributed and active during PDT and PTT tumor treatment. This figure was reproduced from *Nanophotonics*, 2021, **10**, 3161–3168.[57] (d) Converting NIR light to heat to cause PTT cell death. This figure was reproduced from *Pleura Peritoneum*, 2018, 20180124.[56]

used PDT is Type II.[54,55] To generalize, superoxide oxygen (O_2^-) is produced when ROS and oxygen interact. The final goal of cell death will be achieved by transforming oxygen into cytotoxic $^1O_2$, which is caused by PS and $^3O_2$ interaction (Fig. 1(b)).[56]

PTT is a method for phototherapy of malignant tumors, which utilizes photothermal agents (PTAs) to transform light energy into hyperthermia, causing thermal erosion and necrotic death of tumor cells.[58] To investigate thoroughly, the primary mechanism of PTT is this thermal inactivation process, which raises the local temperature by converting light into heat.[59] NIR light is currently the most widely used laser in PTT because NIR light penetrates tissue more profoundly, owing to its lower absorption and scattering properties in tissues. Photothermal substances could convert the absorbed energy of the NIR laser into heat when irradiated, causing cancer cells to die.[60] The simplified schematic of this procedure is illustrated in Fig. 1(d).[56] When light stimulates the PS, an electron moves from the GS to the ^{1}ES. A photon with a longer wavelength and lower energy is released during the straight radiative dissipation from ^{1}ES to GS. This phenomenon is known as fluorescence. It is also possible for the stimulated energy to relax to the GS through non-radiative vibrations. Heat is produced during the relaxation, interceded by motions within the molecules and collisions with neighboring molecules.[59] The heat produced by energy transition zones or plasmon resonance raises the local temperature without harming the remaining healthy tissues. By endocytosing the photothermal materials, it ultimately terminates the tumor cells.[61] Three mechanisms account for the cell's death: denaturation of the tumoral DNA, disruption of angiogenesis, and cell membrane breakdown.[56] Certain PSs apply to both PTT and PDT. Porphyrin-lipid nanovesicles (porphysomes) can be considered an ideal instance in this respect. Both porphysome-PTT and porphysome-PDT have an activation wavelength of 671 nm. In response to 671 nm light, intact porphysomes in the extracellular space undergo photothermal reactions, but disrupted porphysomes within the cell become unquenched and produce ROSs, which can be used in PDT (Fig. 1(c)).[57] PTT offers several advantages, including excellent controllability, O_2 independence, non-invasiveness, and minor adverse effects. However, limitations like poor specificity and restricted light penetration should also be taken into account.[58]

3. A brief outline of porphyrin-comprising MOFs and COFs

A class of tetrapyrrole compounds known as porphyrins comprises substituent groups surrounding a planar porphyrin core. An excellent anchoring site for the complexation of metal atoms is formed by the stable macrocyclic structure of the porphin core. Porphyrin's remarkable photophysical and photochemical characteristics arose from its exceptional energy, hydrogen, and electron transfer capabilities and a high absorption coefficient.[62]

The crucial features of a PS intended for clinical use are chemical stability, the capacity not to aggregate in a buffer. Additionally, it is asserted that PDT is based on the PS's capacity to concentrate specifically in tumor tissue and to induce cells to produce $^1O_2$ and its active radicals when exposed to localized, wavelength-specific radiation. Porphyrin has a highly conjugated core ring structure, similar to that of chlorophyll, and due to its adaptable physicochemical characteristics, it has emerged as one of the most extensively studied PSs. Its important characteristics are its ability to induce tumor cell death through singlet oxygen irradiation, its strong absorption peaks in the visible light range, and its non-injurious nature during therapy. Chemical functionalization, molecular self-assembly, and the formation of PMOFs and PCOFs are frequently employed to increase the electron transfer rate and enhance solar light utilization.[51,63,64]

MOFs have recently garnered more attention as a class of coordination polymers characterized by high porosity, constructed from metal ions and organic linkers. MOFs are mainly classified into seven groups:[65] I. Isoreticular MOFs (a group based on MOF-5, in which the pore functionality and size vary without altering the fundamental cubic architecture). II. Zeolitic imidazolate frameworks (ZIFs) (offer various topologies and are produced utilizing imidazole junctions and transition metal centers). III. Coordination pillared-layer MOFs (possess the characteristics of a minimal assembly size, strong regularity, good design, and straightforward synthesis). IV. Materials of Institute Lavoisier MOFs (produced by combining various transition metal elements with dicarboxylic ligands, like glutaric and succinic acids. They possess desirable T_2-weighted magnetic characteristics and may be used as therapeutic diagnostics). V. Porous coordination networks (comprised of several cubic octahedral nanocages possessing a cage-channel topology in space). VI. UiO series (their microporous structure is three-dimensional, with eight tetrahedral corner cages and an octahedral central pore cage). VII. BioMOFs (they blend biological science and crystalline porous materials. Significant examples of biomolecular ligands are amino acids, peptides, proteins, nucleobases, cyclodextrins, and porphyrins/metalloporphyrins).[65]

MOFs with transition metals have drawn particular interest in the treatment of cancer. In this area, Fe, Cu, and Ti-based materials can be highlighted. Due to their large pore capacity, uniform porosity, and superior biocompatibility, Fe(III)-based MOFs are frequently employed in PTT.[66] An efficient way to increase PTT's effectiveness is to incorporate CuS into the MOF platform's structure. In addition to being a promising photothermal agent for tumor therapy, the Cu-MOF can also be utilized to overcome thermal therapy barriers and facilitate imaging localization, thanks to its adaptable design. In order to make PTT treatment more effective, it can also serve as a link between PTT and other therapies.[67] All Ti-MOFs exhibit good biocompatibility, which makes them excellent options for biomedical applications. A substantial amount of them (whether pure or composition Ti-MOFs)—29% for composites and 50% for pure ones—have been used to cure cancer in recent years.[68]

When treating cancer, MOF-based PDT offered incomparable advantages, including non-invasiveness, low side effects, excellent efficacy, minimal drug resistance, and reduced harm to healthy tissues.[69] Because of their superior performance as PSs in tumor photodynamic treatment, researchers have focused more on porphyrin-comprising MOFs, which use porphyrin molecules as organic ligands. Incorporating porphyrins as PSs into MOFs enhanced the PSs' pharmacokinetic and water solubility characteristics while enabling high loading and delivery to specific tumors. Incorporating porphyrins into MOFs by encapsulating in pores, grafting on the surface to create porphyrin@MOFs, or employing porphyrins as organic linkers to create porphyrin-MOFs not only combines the porphyrins and MOFs' distinctive qualities, but also overcomes some of the drawbacks of porphyrins, including self-quenching due to their rapid agglomeration and low solubility in aqueous environments, low absorption at spectral windows relevant to biology, and poor photochemical stability. This allows for the successful application of porphyrins in biomedicine, particularly in PDT.[70–72]

Another precise and non-invasive tumor treatment technique is sonodynamic therapy. MOF SDT's targeting and ROS conversion capabilities, in turn, improve the cells' capacity to kill cancer. Furthermore, since the majority of sonosensitizers still have the ability to photosensitize, which might enhance tumor treatment, SDT and PDT may work in concert.[73] There are specific compounds that capture the attention of scientists, among others. Researchers advocate tetrakis(4-carboxyphenyl) porphyrin (TCPP) as a standard PS. Through modification and combination, the potent performance of TCPP can be used to create nanotherapeutic agents with superior therapeutic outcomes. Moreover, due to their stable structure, MOFs prevent TCPP from aggregating.[74]

Owing to MOFs' potent properties, TCPP is frequently employed as the foundation of MOFs in conjunction with other medicinal substances to create anti-cancer nanoplatforms that combine the benefits of several therapeutic modalities. For instance, with a combination of $NaLnF_4$ and porphyrinic MOF, 95% of tumors will be effectively eliminated, and the number of cytotoxic T cells will be increased while suppressing distant cells.[75] In the same regard, using multifunctional high boron content MOF nano-co-crystals as a viable substitute for *in situ* brain glioma treatment holds great promise for accurate clinical boron neutron capture therapy for malignancies.[76]

The outstanding role of porphyrinic COFs should not be underestimated. In contrast to MOFs, COFs are organic crystalline substances with pores made of organic monomers with a particular shape bound together by dynamic covalent bonds. With MOFs' intrinsic enhanced specific surface area, porosity, and tunable structure, COFs and MOFs have similar characteristics. Furthermore, given a customizable coordination environment, metal ions could be coordinated into the COF skeleton and could function as active sites upon complete exposure.[77] COFs provide various advantages for cancer therapy: functionalizability, porosity, flexible design, and biocompatibility.[78]

COFs are primarily divided into six categories:[79] I. Boron-based COFs (the advantages of boron bonding in COFs are enhanced thermal stability, low density, and broad surface

area. Nevertheless, the integrity of boron-based COFs' porous frameworks can be destroyed by exposure to water and even mildly humid air). II. Imine-based COFs (Schiff base and hydrazone binding are the two original orders of imine-based COFs. They rely on producing C═N bonds). III. Triazine-bonded COFs (compared to COFs attached to boron, their crystallinity is lower. However, the triazine bonding is responsible for their exceptional chemical and thermal stability). IV. COFs containing triazoles in their structure. V. COFs coupled to azines (hydrogen bonding between the target molecules and the linear azine bond structure may be induced in the pore space. Medicine transfer may benefit from the capacity to combine drug molecules into the structure of these azine-bound COFs through hydrogen bonding). VI. β-Ketoenol-COFs (these COFs exhibit excellent resistance to breakdown when boiling or treating water with acid. Since the stability of these COFs in acidic environments is essential, they could be employed as oral drug carriers because gastric transit is necessary for oral drug administration).[79] Porphyrin units are joined into periodic frameworks in porphyrinic MOFs by metal nodes, including metal ions or clusters. In contrast, porphyrinic COFs have comparable frameworks but are covalently bound to other organic components.[80]

4. Porphyrin-comprising MOF and COF design

MOFs have organic ligands and metal ions linked by coordination bonds, creating a porous structure; porphyrin and its derivatives can be placed in the frameworks as organic ligands or as guests in the structure of MOFs and COFs. Porphyrin can also exist in the structure of COFs, which consists of a covalent bond and is part of the main structure of COFs.[81] With light irradiation on the photosensitizing structure of porphyrin, an electron transfer mechanism occurs, which can lead to the production of $O_2^{\bullet -}$. In another mechanism, direct energy transfer occurs, where molecular oxygen (O_2) is produced, followed by $^1O_2$, which is spontaneously converted into hydrogen peroxide (H_2O_2). This process is harmful to cancer cells and subsequently destroys them.[11] Indeed, the porous structure of MOFs and COFs can encapsulate hydrophobic molecules such as photocatalysts,[82] drugs, organic catalysts, or PSs to increase their stability in water for various applications.[83,84] For example, Masih *et al.* designed a host–guest structure, with the rho-MOF (rho-ZMOF) as a host and platinum metalled porphyrin (Pt(II)TMPyP) as a guest immobilized in the MOF pores, by an *in situ* synthesis method and utilized it for selective anion sensing.[85] In bio-applications, encapsulated porphyrin is prepared using different synthesis methods and post-synthesis to adjust the physicochemical properties of frameworks. In this regard, Ling *et al.* prepared a MOF and used (*meso*-tetra(4-carboxyphenyl)porphyrin) (TCPP) to enhance the catalytic activity. The porphyrin-encapsulated MOF was able to read the signal. The composite FeTCPP@MOF was used to measure and diagnose DNA with high stability and sensitivity and was prepared using the one-pot method.[86] Another method of utilizing the properties of porphyrin in frameworks is designing core–shell structures with controllable shell thickness, which preserves the structure and physicochemical properties and can have good results in phototherapy. To date, many core–shell structures have been studied. In this context, Chen *et al.* designed the UC-COFPt structure, in which the porphyrin-based COF in the shell had photosensitizing properties. The COF pore size, growth, and thickness were controlled. It coated the metal oxide core, leading to the death of more than 80% of the 4T1 cells and shrinking the tumor size after a few days of using 808 nm laser irradiation.[87] Porphyrin combined with the COF can be effectively used in various applications and is resistant to antibiotics due to its photosensitizing properties and ROS generation. A flexible functional membrane prepared by a surface polymerization method by Ding *et al.* shows that the COF using 5,10,15,20-tetrakis(4-aminophenyl) porphyrin (Tph) can have a positive effect by eliminating symptoms.[88]

Cancer cells manage to evade immune recognition and thus escape subsequent destruction. As a safe and complementary method for cancer treatment, immunotherapy can be used, for example, as a component in a carrier that stimulates the immune system, ultimately leading to the attack and increasing death of cancer cells. Previously, immunotherapy was used to treat other diseases.[89] The structure of porphyrin in supramolecular systems, such as MOFs, can enhance this treatment method. Through the loading of biological agents in the porphyrin framework, in addition to PDT, immunotherapy can also be performed at the tumor site. Zhang *et al.* reported that a porphyrin-based MOF (CuTPyP/F68) carrier with biocompatibility, which, according to the properties mentioned earlier, can control the release, stimulate a type of lymphocyte in a cancer cell line, and increase cell death by combining several treatment methods, including PDT and immunotherapy (Fig. 2(a)) by having curcomul (CUR) in the structure, prevented the immune system's biological pathway against the cancer cell to activate antigen-specific T cells.[90] Nanoscale COFs possessing enhanced surface area and elevated PS loading capacity could promise to improve cancer treatment. In addition, other factors related to drug delivery, imaging, and diagnosis can be simultaneously present inside their cavities and act purposefully.

Additionally, due to the biodegradable nature of the COFs, concerns about their toxicity in the body and their metabolism are partially alleviated. COFs can accommodate a wide range of drugs and biological compounds such as antibodies,[92] peptides,[93] and PSs by creating non-covalent bonds, including hydrogen bonds, π–π stacking, or electrostatic interactions. Adding PSs causes phototherapy and increases ROS production in cancer cells. Finally, PDT and PTT induce acute inflammatory responses to alter the tumor microenvironment, potentially enhancing the efficiency of immunotherapy and inhibiting tumor growth and metastasis. COFs are utilized as lightweight compositions and porous scaffolds. Due to their highly conjugated structure and extremely ordered π–π stacking interaction, COFs can form singlet oxygen ($^1O_2$) under laser irradiation.[94]

In this regard, a COF with high porosity and enhanced photostability by creating a strong bond with porphyrin and its derivatives can cause more PSs to accumulate in the structure. COF-618-Cu was reported by Zhang *et al.* to have a crystal

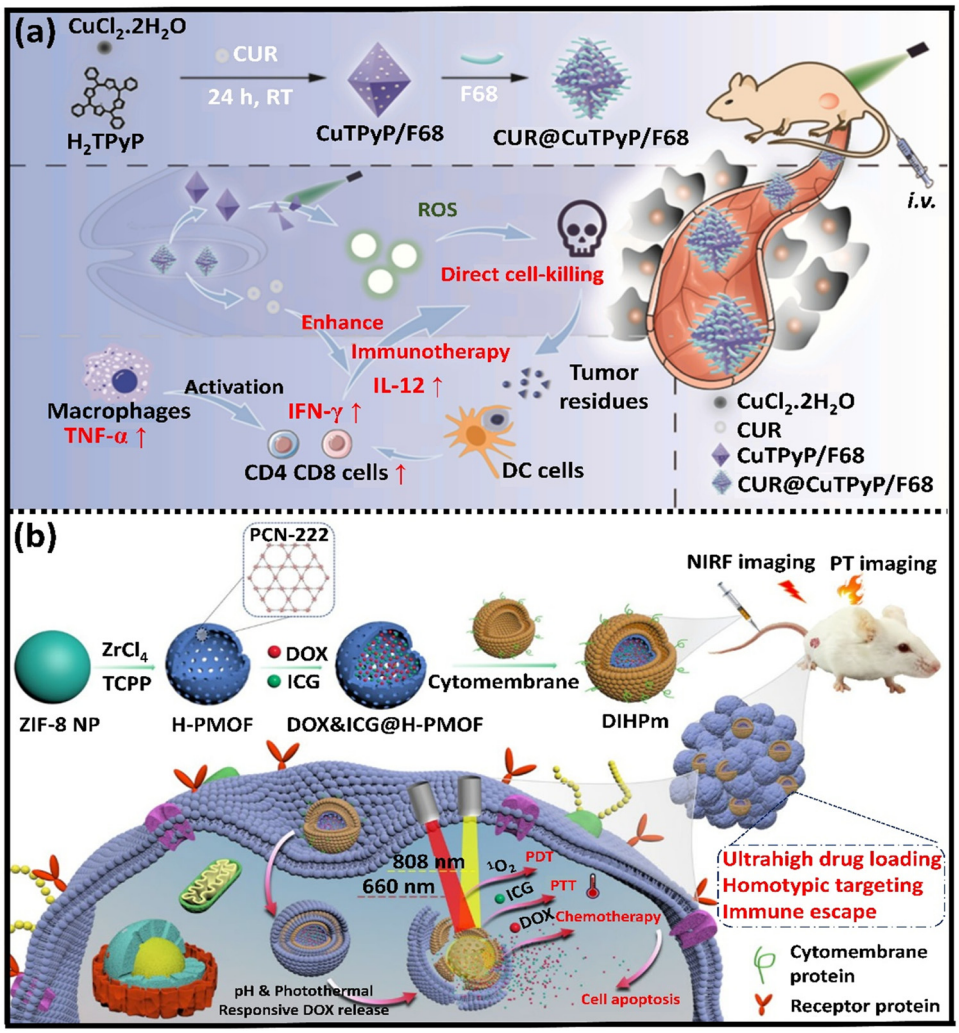

Fig. 2 (a) Schematic of the efficacy of the porphyrin ligand (TPyP) in PDT and the mechanism of CUR@CuTPyP/F68 in immunotherapy treatment and the synergistic effect of CUR with PDT (532 nm/200 mW cm^{-2}, 10 min) on the 4T1 cell line, which had superior tumor targeting and retention capabilities that effectively inhibited tumor growth *in vivo* with just a single dose. This figure was reproduced from *Colloids Surf. B Biointerfaces*, 2022, **214**, 112456.[90] (b) Illustration of the preparation and mechanism of DIHPm inside mouse cancer cells with drug delivery, phototherapy, and imaging. This hollow porphyrin MOF with an ultra-high loading capacity loaded 635% of the drugs Dox and ICG. Ultimately, it increased the rates of apoptosis and necrosis in 4T1 cells. This synergistic effect and triple treatment, even at a very low dose of 2 μg mL^{-1}, could lead to cell death, resulting in only 8% cell survival. This figure was reproduced from *ACS Appl. Mater. Interfaces*, 2021, **13**, 3679–3693.[91]

structure obtained by creating ROS after endocytosis and responding to phototherapy (PDT and PTT), which was able to cause apoptosis, temperature-dependent necrosis, and reduce the CT26 cells' size.[95]

4.1. Preparation approaches of porphyrin-comprising MOFs

MOFs based on porphyrin are also used in other industries due to their regulatory, high capacity, and flexibility.[96] Briefly, MOFs are synthesized using different methods.[97] To date, different synthetic routes have been reported; the most common approaches of MOF synthesis on a nanoscale are solvothermal and hydrothermal methods, which can produce the product in a relatively long time with high temperature and high pressure.[98] The porous structure, high stability, and the ability to integrate various organic and inorganic components enable MOFs to perform well in a wide range of applications. For instance, an iron-based MOF synthesized *via* the solvothermal method has demonstrated enhanced light-activated catalytic performance, attributed to effective coupling, improved charge transfer, and a large active surface area.[99] This possibility of choosing the structures of organic ligands of MOFs can vary according to the need. For example, the metallic element Fe, next to the organic porphyrin ligand or as a single atom within the MOF, can help improve properties. In this regard, Zhou *et al.* recently reported the development of a MOF constructed from porphyrin-derived organic ligands and single-atom Fe centers serving as catalytically active sites. This MOF exhibited high therapeutic efficiency even under hypoxic (low-oxygen) tumor conditions. Upon NIR irradiation, the Fe^{3+} single atoms undergo a valence-state transition, catalyzing the conversion of triplet oxygen ($^3O_2$) into singlet oxygen ($^1O_2$). The results demonstrate a potent PDT effect, amelioration of tumor

hypoxia, and effective tumor ablation, alongside the capability for precise photoacoustic imaging. The strong NIR absorption and narrow band gap of 1.31 eV synergistically contribute to superior PTT conversion efficiency. By providing a robust and catalytically active framework that facilitates efficient light harvesting and ROS generation, the system markedly suppressed tumor growth in murine models and induced significant cytotoxicity against cancer cells.[100]

One of the porphyrin-based MOFs synthesized is $[Cu_2(ZnTcpp)\cdot H_2O]_n$, with the zinc metalated porphyrin derivative 5,10,15,20-tetrakis (4-methoxycarbonylphenyl)porphyrin (ZnTcpp) as the ligand. The composite is capable of causing toxicity in the HCT116 cell line and thus killing colon cancer cells.[101] MIL-101 is synthesized by this method. For example, Cr ions and terephthalate were autoclaved for several hours to prepare the final MOF. Then, zinc porphyrin (Zn[TPP]) was placed in the MOF *via* the encapsulation method for PDT applications.[102] Some methods, such as microwave radiation, can reduce the reaction time.[103,104] If solvent use is limited, a method such as mechanochemical grinding can be applied. Electrospinning can be a simple and highly reproducible approach to produce MOFs.[105,106] By using soft templates such as cetyltrimethylammonium bromide (CTAB) and hard templates such as graphene and metal oxides, patterns can be prepared in which MOFs are synthesized in a controlled manner, and after synthesis, the templates are removed to obtain the final product.[107,108] Other methods, such as the sonochemical method and electrochemical routes, are also used, each with advantages.[109] PCN-224 is one of the MOFs that features porphyrin in its structure as a ligand, composed of tetrakis (4-carboxyphenyl) porphyrin (H_2TCPP) and Zr metal, with spherical morphology and surface functional groups suitable for conjugation with biological structures for targeting. Therefore, a DNA-targeted porphyrin-based MOF was prepared and demonstrated high cytotoxicity.[110] The solvothermal synthesis method and self-assembly phenomenon can cause the formation of a MOF-based carrier that has a PS. Therefore, a mesoporous structure with ZIF-8 coated with the tetrakis(4-carboxyphenyl)porphyrin (TCPP) structure combined with PCN-222 MOF was reported. An H-PMOF was loaded with an enhanced capacity for indocyanine green (ICG) and DOX drugs, which possess anti-tumor properties. The (DOX&ICG)@H-PMOF@mem (called DIHPm) biomimetic nanoplatform is afforded by a cancer cell membrane camouflage of the (DOX&ICG)@H-PMOF composite nanoparticles that exhibited a remarkable imaging-guided synergistic PDT/PTT/chemotherapy anticancer activity with low systemic toxicity. The DIHPm nanoplatform increased the rate of apoptosis in 4T1 cells (Fig. 2(b)).[91]

Qarehdaghi *et al.* demonstrated that GO can serve as a suitable pH-responsive substrate. However, the unique properties of MOFs can be effective in preparing a smart carrier. The Cu-TCPP MOF, synthesized *via* a one-pot solvothermal solution approach using a Cu node and an organic porphyrin ligand, can prevent GO accumulation in the liver by creating a positive superficial charge and increasing the time of staying in blood circulation and endocytosis. Therefore, this biocompatible carrier is reported to release 98% DOX in the acidic milieu of tumors, which can induce cell death in various cell lines.[111]

Some porphyrin derivatives used in producing MOFs as organic ligands are shown in Fig. 3.[104] Table 1 presents the recently prepared porphyrin-comprising MOFs used in phototherapy. PMOFs are a group of substances that have diverse applications due to their porous structure and unique properties. One of the best-known examples is the PCN series of MOFs, which are made using a tetrafunctional porphyrin ligand ($TCPP^{4-}$) and zirconium clusters. PMOFs have advantages over single porphyrin molecules, including tunable pore size, a high specific surface area, and the possibility of chemical modification of ligands. They also exhibit high chemical and thermal stability, allowing for reuse without loss of performance, making them highly suitable for industrial applications. Studies show that two widely used PMOFs, PCN-224 and PCN-222, have significant specific surface areas of 2214 and 1409 $m^2\ g^{-1}$, respectively (using N_2 adsorption at 77 K). BET analysis also confirms the presence of distinct pores in these structures, as observed in the research. PCN-222 has a mesoporous structure with a pore diameter of 3.4 nm, attributed to its rindless 3D open channels. It also contains micropores with a diameter of 0.9 nm. In contrast, PCN-224, due to its lower coordination number of its metal cluster, creates a 3D open channel with a diameter of approximately 1.9 nm. Optically, PMOFs have outstanding photophysical performance. Their structures are designed to absorb visible light and excite electrons in the porphyrin center, leading to strong light emission through fluorescence or phosphorescence. The topology of PMOFs has a significant impact on their fluorescence behavior. Studies have shown that, upon optical excitation at a wavelength of 420 nm, these structures exhibit two fluorescence peaks in the red region of the spectrum, which are attributed to molecular vibrations. The fluorescence intensity in different PMOFs depends on the orientation and spacing of the porphyrin units within their structure, which affects the efficiency of processes such as singlet–singlet annihilation. A correlation between fluorescence intensity (Φ_{fluo}) and excited state lifetime (τ_{fluo}) has also been observed, such that structures with stronger fluorescence have longer lifetimes. This trend is clearly related to the topology of PMOFs, and the order of fluorescence efficiency is reported as $TCPP^{4-}$ > PCN-223 > MOF-525 > PCN-224. The difference between $TCPP^{4-}$ and other PMOFs is attributed to the heavy atom effect of the Zr metal ion. In addition to 3D PMOFs, there are also 2D structures, sometimes referred to as metal–organic networks, which exhibit different optical properties than their 3D counterparts.[112] Three zirconium–porphyrin frameworks, designated as PCN-222, PCN-223, and PCN-224 with different structures based on Zr_6 clusters and quadruple TCPP linkers, show remarkable chemical stability in aqueous environments and a wide pH range. The main difference between these frameworks lies in the number and type of connections between Zr_6 clusters and the linkers; PCN-222 has a csq topology with eight linkers per cluster, while PCN-223 and PCN-224 have six and twelve connections, respectively. Evaluation of the acid stability of these MOFs in various sulfuric acid solutions revealed that PCN-224 has the least resistance to attack by water and acid molecules due to the presence of more structural defects. In contrast, PCN-222 and PCN-223, with a

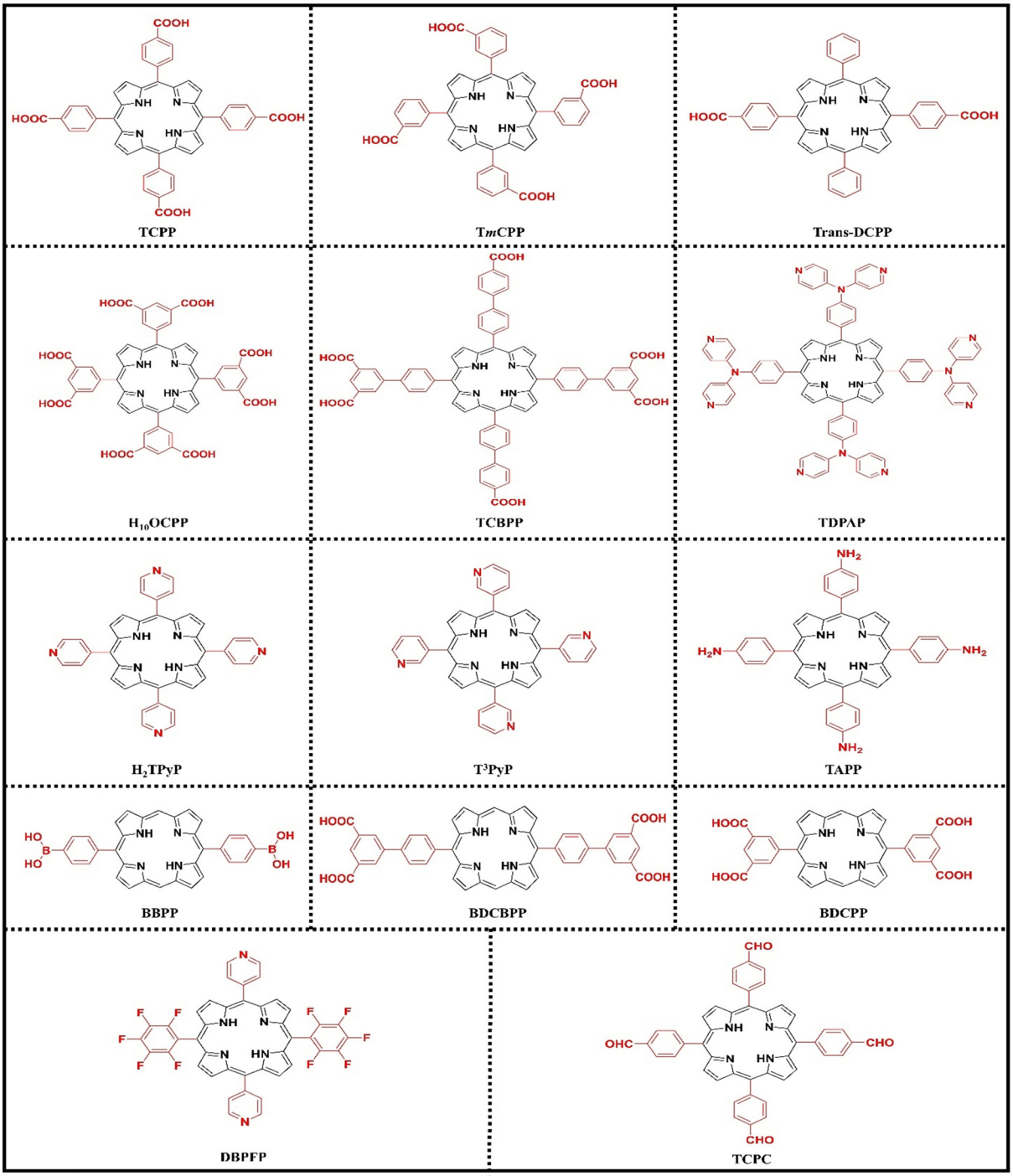

Fig. 3 Some porphyrinic ligands used in MOFs. Due to the different bonds between porphyrins and metal ions/clusters in PMOFs, MOFs can be classified into porphyrin MOFs and porphyrin@MOFs. Abbreviations: 5,10,15,20-tetrakis(4,4′-bispyridylaminophenyl)porphyrin (TDPAP), 5,10,15,20-tetrakis(3-pyridyl)porphyrin (T_3PyP), 5,15-bis(dicarboxyphenyl)porphyrin (BDCPP), 5,15-dipyridyl-10,20-bis(pentafluorophenyl)porphyrin (DBPFP), 5,10,15,20-tetrakis(4-bishydroxyboryl)porphyrin (BBPP), 5,10,15,20-tetrakis(3,5-biscarboxyphenyl)porphyrin ($H_{10}OCPP$), 5,15-di(4-carboxyphenyl)-10,20-diphenylporphyrin (*trans*-DCPP), and tetrakis(3-carboxyphenyl)porphyrin (TmCPP). This figure was reproduced from *Coord. Chem. Rev.*, 2021, **439**, 213945.[104]

more coherent structure and fewer defects, exhibit higher stability and maintain their crystallinity after immersion in 0.20 M sulfuric acid. However, limited structural defects can enhance the adsorption of sulfate species (SO_4^{2-}) into the framework, which is beneficial for some applications.[113]

4.2. Preparation approaches of porphyrin-comprising COFs

COFs as light crystalline structures are utilized in various industries due to their lightness and stability of covalent chemical bonds. In addition to these features, COFs are utilized in phototherapy due to their large pore size, low toxicity, and

Table 1 Porphyrin-containing MOFs that have been prepared recently for phototherapy

Entry	MOF	Ligand	Metal node	Application	Cell line	Composite	Light source	*In vivo*/*in vitro* results	Ref.
1	FeTPt[a]	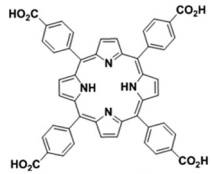 TCPP[b]	Fe^{3+}	PDT/drug delivery	4T1 cells	FeTPt@CCM[c]	PDT (670 nm/ 100 mW cm^{-2})	57.4 ± 4.81% cellular apoptosis	114
2	Hf-TCPP	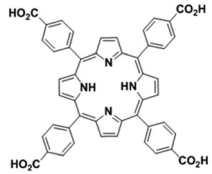 TCPP	Hf^{4+}	PDT/radiation therapy	4TI/HeLa human cells/NIH3T3 mouse	Hf-TCPPNMOF-PEG[d]	PDT (661 nm/5 mW cm^{-2})	Highest level of tumor cell destruction	115
3	PCN[e]-224 ZIF-8 (MOF@MOF)	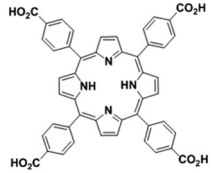 TCPP	Zr_6/Zn^{2+}	PDT/drug delivery	SiHa cells	7ACC2[f]/ DOX@PCN-224	PDT (660 nm/ 200 mW)	70% reduction in tumor growth	116
4	PCN-224	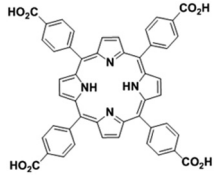 TCPP	Zr^{4+}	PDT/drug delivery	CT26 cells	PCN-224@MOS[g]-DOX	PDT (660 nm/ 0.3 W cm^{-2})	The tumor volume reached 1/3rd of its original volume after 16 days	117
5	HKUST-1-Zn (MOF-199)	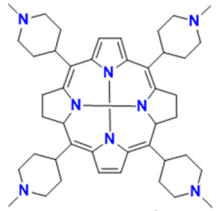 TMPyP[h]	Zn^{2+}	PDT/ theranostics	HeLa cells	PS@MOF	PDT (660 nm/ 100 mW cm^{-2})	53.91% apoptosis cells	118

Table 1 (*continued*)

Entry	MOF	Ligand	Metal node	Application	Cell line	Composite	Light source	*In vivo*/*in vitro* results	Ref.
6	PCN-224	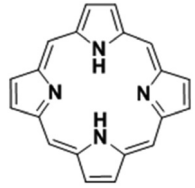 Porphyrin	Zr_6 cluster	PDT/drug delivery	CT26 cells	UCNP[i]-MOF	PDT (980 nm/ 1.2 W cm^{-2})	Reduction in the number of viable tumor cells after 14 days (28.9%)	119
7	PCN-224	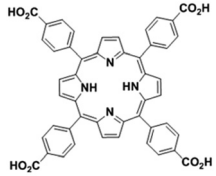 TCPP	Zr^{4+}	PDT	HeLa cells	FA[j]-PCN-224	PDT (630 nm)	The best PDT efficacy: 81% for the results of cellular uptake	120
8	Hf-UiO-AM	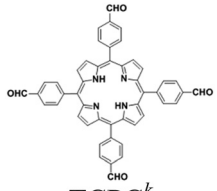 TCPC[k]	Hf^{4+}	PDT/PTT/ imaging	HeLa cells	HUC-PEG	PDT (671 nm/ 0.6 W cm^{-2})	Tumor inhibition rate up to 88.4%	121
9	TCPC-UiO-66	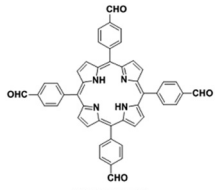 TCPC	Hf^{4+}	PTT/imaging	HepG2 cells	TCPC-UiO	PTT (635 nm/ 0.8 W cm^{-2})	More than 80% of HepG2 and HeLa cells and 70% of 4T1 and MCF-7 cells are dead	122
10	DBP-UiO	 H_2DBP[l]	Hf^{4+}	PDT	Head and neck cancer	DBP-UiO	PDT (640 nm/ 100 W $cm^{-2)}$	Significant fractions of tumor cells were undergoing apoptosis/ necrosis	123

Table 1 (*continued*)

Entry	MOF	Ligand	Metal node	Application	Cell line	Composite	Light source	*In vivo*/*in vitro* results	Ref.
11	DBC^{m}-UiO	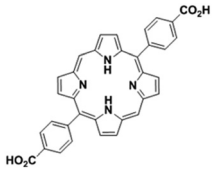 H_2DBP	Hf^{4+}	PDT	Colon cancer	DBC-UiO	PDT (650 nm/ 0.1 W cm^{-2})	50% mortality at concentrations ($>$20 μM) of ligand	124
12	PCN-222	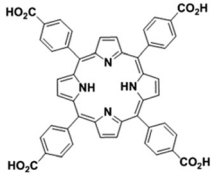 TCPP	Zr^{4+}	PDT	CT26 cells	Pda^{n}-Pt@PCN-FA	PDT (660 nm)/ (30 mW cm^{-2})	High cytotoxicity (nearly 80%)	125
13	CuTPyP	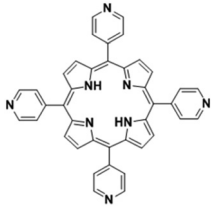 H_2TPyP^{o}	Cu	PDT/ chemotherapy	Breast cancer	F68-DOX@CuTPyP	PDT (532 nm, 200 mW cm^{-2})	Strong apoptosis-inducing effect	126
14	FeTCPP	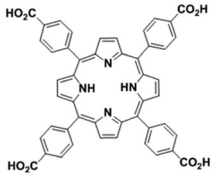 TCPP	Fe^{3+}	PDT/ chemotherapy	KB cells	FeTCPP/Fe_2O_3	PDT (660 nm/ current of 1.5 A)	The percentage of surviving KB cells decreased to 18.61%	127
15	PCN-224	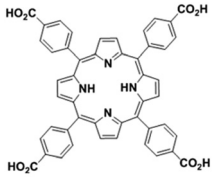 TCPP	Zr	PDT	4T1 cells	HP-MOF^{p}	PDT (660 nm)	Tumor inhibition 68.1%	128

Table 1 (*continued*)

Entry	MOF	Ligand	Metal node	Application	Cell line	Composite	Light source	*In vivo*/*in vitro* results	Ref.
16	PCN	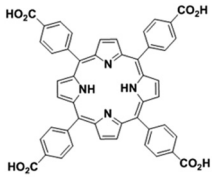 TCPP	Zr^{4+}	PDT	HeLa cells	TPP-UCNPs@MOF-Pt	PDT (980 nm/ 1.5 W cm^{-2})	Increased tumor growth inhibition	129
17	PCN-224	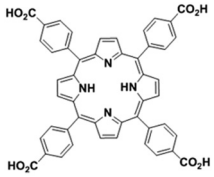 TCPP	Zr_6 cluster	PDT	4T1 cells	MOF-GOX[q]-cancer cell membrane (mCGP[r])	PDT (660 nm/ 29.8 mW cm^{-2})	Cancer inhibition of more than 80%	130
18	TBP-MOF	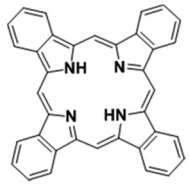 TBP^{s}	Zr_6 cluster	PDT/ immunotherapy	4T1 cells	Benzoporphyrin-based MOF (TBP-MOF)	PDT (660 nm/30 mW cm^{-2})	Significant reduction in tumor volume after 15 days	131
19	PCN-224	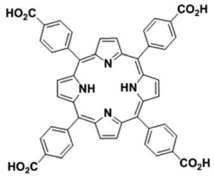 TCPP	Zr6 cluster	PDT	HeLa cells	MOF@QD[t]	PDT (650 nm)/ (1 W cm^{-2})	High tumor toxicity and easy renal clearance	132
20	PCN-224	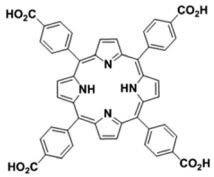 TCPP	Zr	PDT	4T1 cells	PC20-MOFs[u]-FA	PDT (808 nm/ 1 W cm^{-2})	Strong therapeutic effect	133

Table 1 (*continued*)

Entry	MOF	Ligand	Metal node	Application	Cell line	Composite	Light source	*In vivo*/*in vitro* results	Ref.
21	Cu-TCPP	TCPP	Cu	PDT/imaging	Saos-2 cells	Cu-TCPP MOF	PDT (808 nm/ 1 W cm^{-2})	Increase in mortality by about 90%	134
22	UiO-AM	NH_2-BDC^{v}	Zr	PDT	HeLa/HepG2 cells	MOF@POP^{w} (UNM)	PDT (450 nm/30 mW cm^{-2})	The ratio of apoptotic cells is 80.7% for 15 minutes (time-dependent anticancer efficacy)	135

^{a} Fe^{3+}, *meso*-tetra(4-carboxyphenyl)porphine and oxaliplatin prodrug. ^{b} *Meso*-tetra(4-carboxyphenyl)porphyrin. ^{c} Cancer cell membrane. ^{d} TCPP nanoscale MOF with polyethylene glycol. ^{e} Porous coordination network. ^{f} 7-amino carboxycoumarins-2. ^{g} Mesoporous organic silica. ^{h} Tetrakis(1-methylpyrimidinium-4-yl)porphyrin. ^{i} Upconversion NPs. ^{j} Folic acid. ^{k} Tetrakis(4-carboxyphenyl)chlorin. ^{l} 5,15-Di(*p*-benzoato)-10,20-diphenyl-porphyrin. ^{m} 5,15-Di(*p*-benzoato)-chlorin. ^{n} Polydopamine. ^{o} 5,10,15,20-Tetra(4-pyridyl)porphyrin. ^{p} Hierarchically porous MOFs. ^{q} Glucose oxidase. ^{r} Membrane glucose oxidase. ^{s} Tetrabenzoporphyrin. ^{t} Quantum dot. ^{u} Porphyrin/cypate-based MOFs (PC-MOFs). ^{v} 2-Aminobenzene-1,4-dicarboxylic acid. ^{w} Porous organic polymers.

facile surface functionalization of targeting ligands for targeted delivery systems.[19] COFs possess rich π-conjugated structures and can be modified easily, making them appropriate for diverse drug molecule loading *via* host–guest interaction, weak bonding (hydrogen bonding, electrostatic, and π–π stacking), and other methods. COFs are synthesized by various approaches, including formation of triazine reaction and boronic ester reaction, formation of amides, and porphyrinoid COFs with different symmetry-dependent topologies reported previously. Briefly, the synthesis of NPs is done using two approaches, from top to bottom and from bottom to top, and COFs in nanoscales are no exception to this rule. The ultrasound method is employed in a top-down approach in COF synthesis with chemical exfoliation to control the surface. Alternatively, porphyrin COFs can be synthesized using a suitable surfactant to control the thickness through a bottom-up approach, known as the interfacial synthesis method.[19,136] Fig. 4 shows the porphyrin monomers that can be applied in preparing porphyrin-containing COFs.[136]

For example, Wan *et al.* used the solvothermal method to obtain COF-366 and COF-66 with different space groups for charge carrier mobility usage, thereby utilizing the rings within the porphyrin structure and the π–π stacking created in the structure.[137] The light irradiated on the COF can create holes in the capacitance band that have a lot of energy in the excited state. This energy is released as heat, allowing it to return to a stable and relaxed state. The heat generated can reach the tissues adjacent to the COF. With this strategy, when the photosensitizing COF structure is placed in the cell and exposed to light with a particular wavelength, it causes heat and cell apoptosis. When combined with another treatment method, such as drug delivery or PTT, the result is more effective, and the probability of cancer cell death increases.

This makes it possible to use the COFs in the drug's controlled release to release it into the environment by creating heat, and the amount of normal cell damage is diminished. Additionally, PTT causes the release of tumor antigens, stimulating the immune system.[138] Feng *et al.* designed the mPPy@COF-Por core–shell structure, in which the PPy@COF core structure is comprised of polypyrrole (PPy). Then the prepared COF was coated over the core. In this design, porphyrin is placed on the shell structure as a PS. So the shell is further decorated with (5-(4 aminophenyl)-10,15, 20-triphenyl porphyrin) (Por), which is a known PS, and then coated with a membrane made of HTC116 cancer cells to act in a targeted manner. To improve the performance of PDT, light with a wavelength of 660 nm was used to observe the production of ROS. But for the production of heat and cell damage caused by heat, light with a wavelength of 808 nm was used. The combination of these two treatment methods led to better results than when one method was used, *i.e.*, cell apoptosis with minimal side effects (Fig. 5).[139]

As mentioned, both MOFs and COFs are porous structures with large surface areas and can be designed with specific main frameworks and pore sizes. However, their structural differences lead to unique properties that are highly significant in various applications, particularly in the fields of drug delivery and medicine. MOF structures are formed through coordination

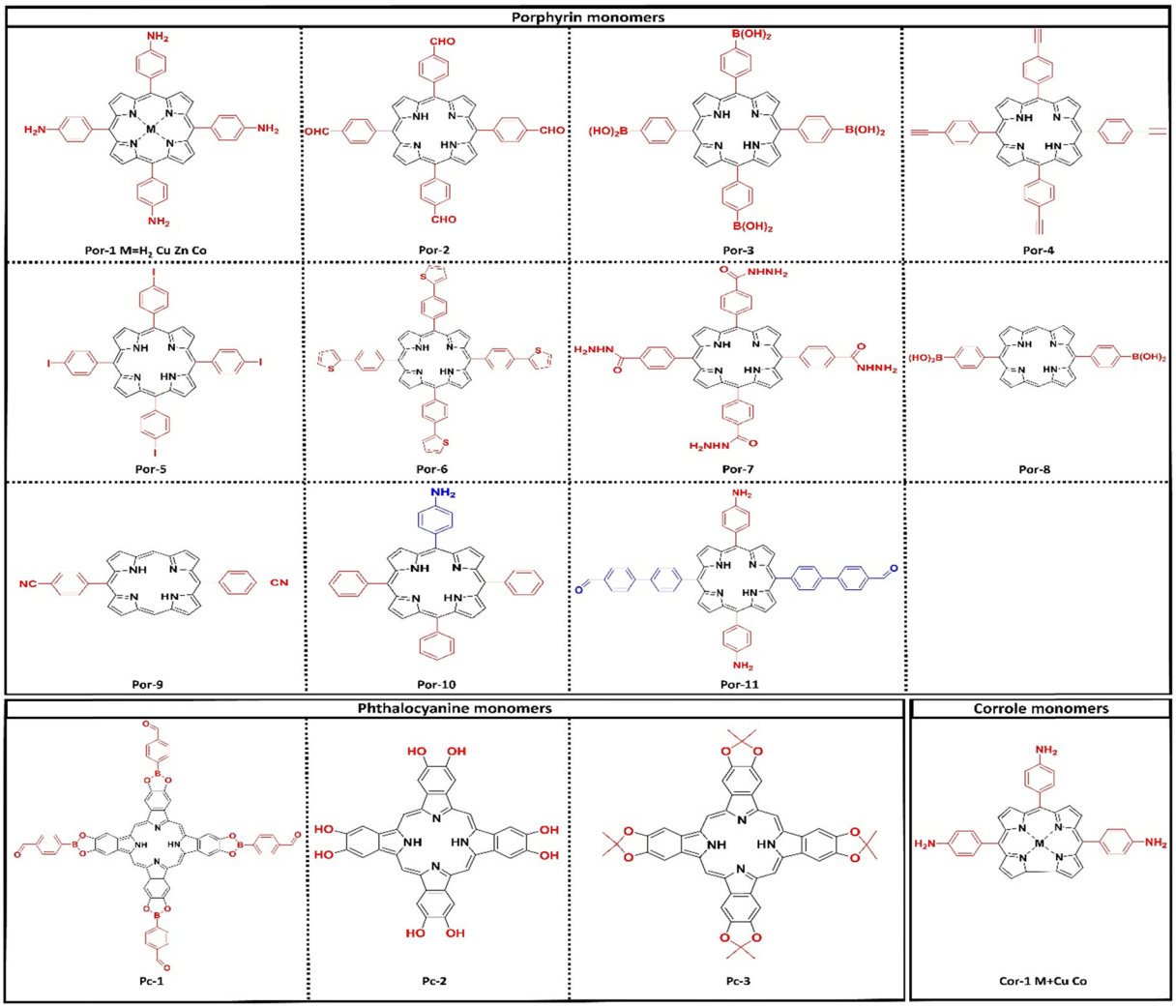

Fig. 4 Types of monomers that are used to prepare COFs by creating covalent bonds. Derivatives of porphyrin (Por-1-11), phthalocyanine (Pc-1-2), and corrole (Cor-1) containing aldehyde, amino, boronic acid, terminal alkyne, bromo, hydroxy, and thienyl groups. This figure was reproduced from *Coord. Chem. Rev.*, 2021, **435**, 213778.[136]

interactions between organic ligands and metals, whereas COF structures are based on strong covalent bonds. The type of bonding directly influences the physical properties of a chemical structure. Therefore, given the nature of the bonds in these two frameworks, the mechanical strength and high resistance of COFs can be reliably anticipated. In various applications (especially drug delivery and therapy), the stability of nanocarriers is critically essential. In applications where the presence of MOFs inside the body is required, such as in PTT combined chemotherapy, where the porphyrin properties of MOF structures are utilized, the stability of MOFs under different pH conditions becomes critical. Some MOFs synthesized at varying pH levels exhibit various degrees of resistance and structural stability. When comparing MOFs and COFs, the strong covalent bond in COFs suggests that they can possess greater resistance and stability. Naturally, there are significant differences in the synthesis methods of these two structures. For instance, in the synthesis of aerogel MOFs, metal salts and organic ligands are dissolved in a solvent to form coordination bonds. In such structures, the choice of ligands and metal ions can influence the resulting density. In contrast, the synthesis of aerogel COFs involves dissolving organic monomers, followed by a condensation reaction that forms covalent bonds. The absence of metal ions in COFs generally results in lower densities compared to MOFs. Therefore, based on their different bonding mechanisms, MOFs and COFs may exhibit distinct stability and biodegradability profiles in various environments, particularly within biological systems.[140,141]

The presence of metal ions in MOFs differentiates them from COF structures that are generally composed of light elements (H, O, N, and C). In *in vivo* applications, the presence of heavy metals or metal ions is significant. Cytotoxicity is controlled by various factors such as surface charge and types of specific interactions between MOFs and cells, for example, through the release of metal ions, which COFs do not have in their structure.[142,143] The use of the porphyrin structure poses challenges. This is due to the low solubility of the porphyrin structure in aqueous solutions, resulting from the strong π–π interactions between the planar polyaromatic macrocycles. The formation of covalent bonds in

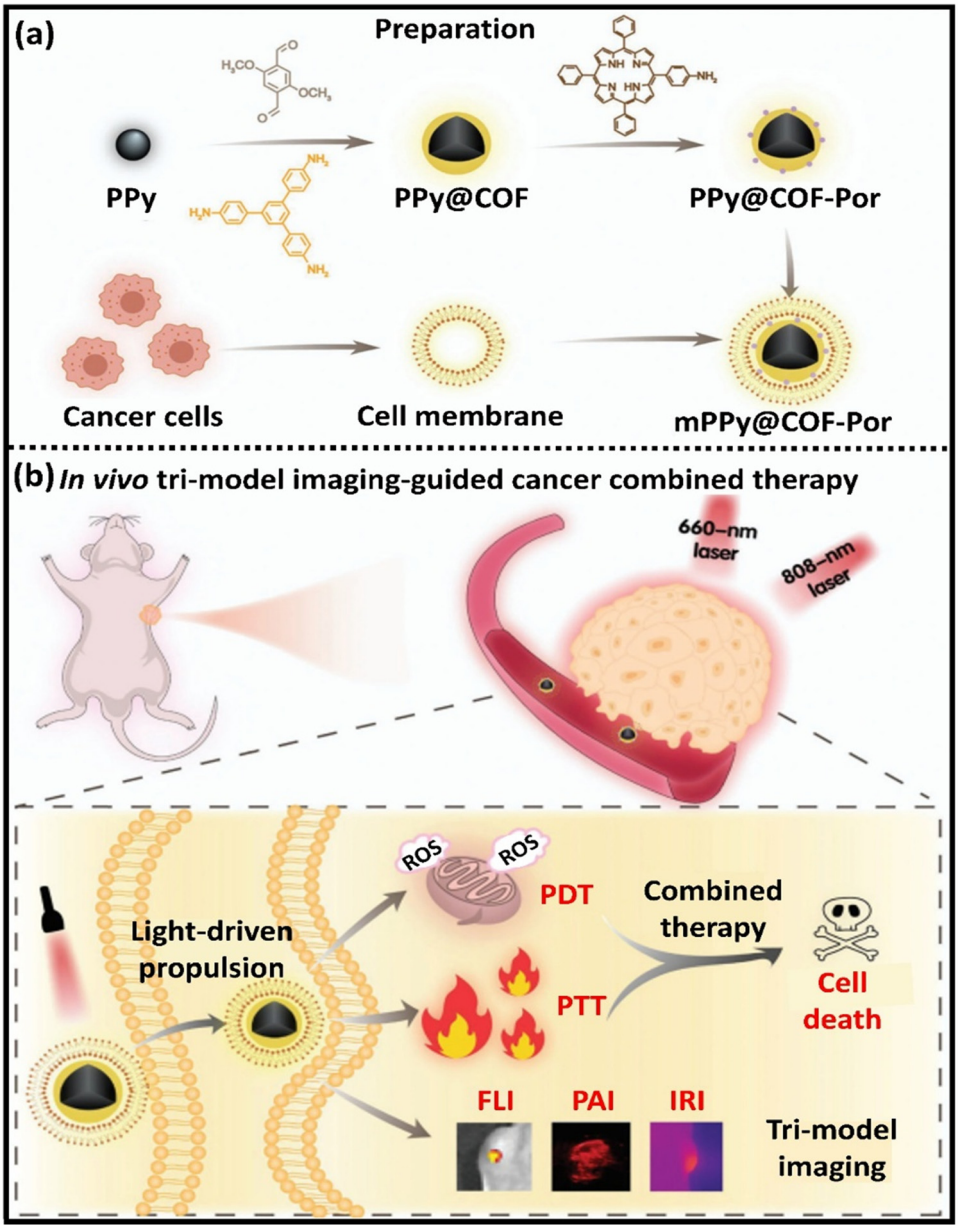

Fig. 5 (a) Preparation of the PPy@COF-Pro structure and (b) the performance of the final core–shell motor *in vivo* on the Veri cell line *HTC116* under 660 nm light irradiation (50 mW, cm^{-2}) and investigation of the effect of PTT and PDT in the treatment process and tumor growth inhibition and cell adhesion, cellular uptake, and cell penetration behaviors of the mPPy@COF-Por nanomotor. This figure was reproduced from *Adv. Healthc. Mater.*, 2023, **12**, 2301645.[139]

porphyrin molecules leads to electron transfer between their different monomers. Therefore, PCOFs could be a way to overcome this limitation and increase the efficiency of electron transfer, as well as create specific reactions. They also facilitate the creation of ligands on the porphyrin ring.[144] PCOFs with strong stability can exhibit excellent biological interactions. Additionally, considering the toxicity of the metal type and the necessary safety precautions, MOFs can be utilized to advantage in drug delivery, as the properties of porphyrin significantly contribute to the treatment of cancer cells. Aromatic PMOFs result in strong light absorption, and the intrinsic properties of porphyrin are preserved in high surface area MOFs, and chelation of metal ions allows the binding of small molecules to the porphyrin.[145]

If, in a treatment method, serious damage is not done to the cancer cell or cancer cells remain, it can cause metastasis and regrowth of the tumor, and the treatment method is incomplete; therefore, a suitable treatment can reliably eliminate the tumor. For instance, combined methods create heat, ROS, or damage to the tumor cells' DNA, thereby reducing the probability of metastasis. Therefore, Tai *et al.* prepared a MOF with a Zr element and the TCPP ligand, whose cage-like structure can accommodate many other molecules or drugs and damage

Table 2 PCOFs have been developed in recent years for phototherapy applications

Entry	Composite	Application	Effective treatment factors	Light source	Cell line	*In vivo*/*in vitro* results	Ref.
1	HPCOF[a]	PDT/PTT/imaging	Porphyrin	PTT (808 nm, 1 W cm^{-2}) PDT (660 nm, 450 mW cm^{-2})	4T1	Tumor growth was completely inhibited and eliminated.	147
2	COFNDs[b]-PEG	PDT	Porphyrin	PDT (638 ± 10 nm, high power)	HeLa	Inhibit tumor growth and facilitate kidney cleansing	148
3	CTP	PTT/SDT[c]	Porphyrin Sonosensitizer	SDT (1 MHz, 1.5 W)	4T1	The tumor underwent apoptosis.	149
4	MnO_2/ZnCOF@Au&BSA[d]	PTT/delivery system/imaging	Porphyrin Metal NPs	PTT (808 nm, 1 W cm^{-2})	HepG2	Tumor inhibition rate of 79.5%	150
5	Se@COF-PEG	PDT	Porphyrin TCP	PDT (635 nm, 0.2 W cm^{-2})	4T1	Complete destruction of the tumor	151
6	HA[e]@COF NSs	PDT target	Porphyrin/HA	PDT (633 nm, 0.2 W cm^{-2})	HepG2/MC7	Tumor growth inhibition and induction of apoptosis after 14 days	152
7	AQ4N[f]@$THPP_{TK}$-PEG	PDT/chemotherapy	THPP[g]/AQ4N	PDT (660 nm, 50 mW cm^{-2})	4T1/HeLa/L929	Significant reduction in tumor volume after 14 days	153
8	Cu-Dha[h]Tph[i]	PTT/PDT	Porphyrin/H_2S	PTT (808 nm, 2 W cm^{-2}) PDT (660 nm, 50 mW cm^{-2})	HCT116	Almost all tumor tissue was eradicated, demonstrating synergy and great benefits of combination therapy over monotherapy.	154
9	PCOP[j]	PTT/PDT	Tph[k]	PTT (808 nm, 0.9 W cm^{-2}) PDT (650 nm, 100 mW cm^{-2})	HeLa	High photothermal conversion efficiency (21.7%) and inhibition of tumor growth	155

[a] Hypoxia-triggered degradable porphyrinic COF. [b] Nanodots. [c] Sonodynamic therapy. [d] Bovine serum albumin. [e] Hyaluronic acid. [f] Hypoxia-responsive prodrug banoxantrone. [g] Tetra(4-hydroxyphenyl)porphine. [h] 2,5-Dihydroxyterephthalaldehyde. [i] Tetra(*p*-aminophenyl)porphyrin. [j] Porphyrin-containing covalent organic polymers. [k] 5,10,15,20-Tetrakis(4-aminophenyl)porphine.

cancer cells using the PDT method. Next, the COF structure was coated on the MOF to protect the core (MOF with PS) and achieve high drug loading efficiency. Due to the presence of several active sites on the COF surface, it can react with other structures. In this composite, a poloxamer was used due to its high solubility. The new structure of ZTN@COF@poloxamer under 660 nm laser irradiation can be an effective treatment agent by generating ROS in cancer cells and damaging cancer cell DNA, reducing tumor size, preventing metastasis, and activating the immune system.[146] Table 2 presents the recently prepared porphyrin-comprising COFs used in phototherapy.

5. Porphyrin-comprising MOFs and COFs in phototherapy

Improved photophysical properties are offered by porphyrin-based species as organic dyes; nevertheless, there are serious obstacles in the way of using them as highly efficient PSs for PDT, such as their low cell permeability, aggregation tendency, poor water solubility, and $^1O_2$ self-quenching. These problems can be effectively resolved by using COFs and MOFs. The photodynamic effects of PSs can be improved, and their quenching can be decreased by loading them into nanoscale MOFs. In addition, due to their large interior pores and free active terminal groups (bonding defects), COFs have developed into ideal carriers for loading hydrophobic PSs and photothermal agents.[12,156] PTT also has an excellent opportunity for research and development. This possibility arises from combining the chemotherapeutic effect of MOF's drug-carrying capability with the thermal ablation of tumors induced by the conversion capabilities of MOF materials, which absorb light energy in the NIR range and convert it into thermal energy.[157]

5.1. Photodynamic therapy

Porphyrin-comprising MOFs, whose porous architectures promote an enhanced porphyrin loading content and an accelerated diffusion of ROS, have emerged as ideal nano-PSs for PDT. They also feature configurable porosity, customizable chemical compositions, and controllable morphologies.[158] Through the intersystem crossing (ISC) process, the excited porphyrin could transform into an excited triplet (T_1) state. From there, it can either transfer its energy to molecules of O_2, producing highly cytotoxic $^1O_2$ (type II) or generate $O_2^{\bullet-}$ and $^\bullet$OH with the reaction of the surrounding H_2O or O_2 by an electron transition procedure (type I), as shown in Fig. 6(a).[80]

By effectively preventing the unexpected π–π stacking of the porphyrin motifs, MOF structures can improve the ISC from the singlet excited state to the T_1 state, increasing PDT efficacy.[80] Porphyrin-based two-dimensional (2D) MOFs have been investigated for the PDT treatment of breast cancer in the clinical treatment of hypoxic tumors. Of particular interest are 2D nanosheets, which have enormous specific surface areas and distinctive physical and chemical properties. The type I mechanism of PDT is used to treat cancer using a variety of 2D NPs as nanomedicines in normoxic circumstances. Nonetheless, several 2D MOF nanosheets are being used as type I PDT medications to treat cancer and combat hypoxia.[161]

COFs with customizable structures would be the best choice for precisely managing exciton dissociation and transformation, as they considerably ease the manipulation of structures and excitonic effects. According to an investigation, excitons

and charge carriers coexist in the metal-free COF when exposed to radiation. Adding different metal ions disrupts this equilibrium, significantly altering the exciton's behavior. To be more precise, the porphyrin center's Zn^{2+} could effectively transform singlet to triplet excitons, speed up the energy transition procedure, and activate O_2 molecules to create $^1O_2$. In contrast, the Ni^{2+} present in the porphyrin center facilitates the charge transfer procedure and speeds up exciton dissociation to carriers, producing $O_2^{\bullet -}$ from O_2.[162]

Based on the generation method, ROS are separated into two categories and are considered potential green oxidants. The hydroxyl radicals ($^{\bullet}OH$), superoxide radicals ($O_2^{\bullet -}$), and hydrogen peroxide (H_2O_2) are examples of type I ROS that are produced directly through electron transfer (*via* exciton dissociation) by an electronically excited PS from substrates. $^1O_2$ is produced by type II ROS, which is thought to result from an energy transfer mechanism involving the transition of triplet GS molecular oxygen ($^3O_2$) into its very reactive singlet form.[163] Fewer ROS are produced by regular PSs, and their performance in photothermal conversion is not perfect. These problems arise from their aggregation in aqueous solution, which quenches their fluorescence (a process known as aggregation-caused quenching) and breaks down during laser irradiation (photobleaching). Nonetheless, a few new PCOFs exhibit a distinct staggered stacking mode and are designed to lessen the impacts of aggregation-caused quenching and photobleaching.[95]

Multi-porphyrin arrays are attention-grabbing molecules that have two or more porphyrin units covalently or noncovalently bonded together to produce homogeneous single molecular structures. *In vivo*, PDT can benefit from the structure-dependent biological benefits that the synthetic multi-porphyrin arrays can provide, in addition to the intrinsic porphyrin capabilities. It is relevant to mention that the creation of multi-porphyrin arrays has been demonstrated to partially boost excited-state energy migration and GS hole/electron hopping, which may advance the compounds' use as photodynamic agents for antimicrobial or cancer treatments.[80]

One of the primary parameters limiting the efficacy of PDT is the absence of oxygen in solid tumors. Hypoxic tumor regions have two beneficial ways: on one hand, they promote tumor growth and metastasis, and on the other hand, they lessen the tumor tissues' reactivity to PDT and other therapies like radiation and chemotherapy. As a result, managing hypoxia is preferable and is currently a prevalent research issue in both the clinical and academic domains.[164] Oxygen-independent PDT has been widely investigated recently, and some efficient methods have been suggested. Targeting and enhancing PDT efficacy is the goal of a porphyrin-based MOF in conjunction with hyaluronate-modified CaO_2 NPs. Here, the hypoxia issue is resolved by the reaction of CaO_2 with H_2O or mild acid, which produces O_2.[165]

Using a multicarboxyl modification technique to manufacture a multifunctional porphyrin-based MOF can be considered another proposed solution. A report on a new self-oxygen formation improved photodynamic platform is provided, along with verification of its anti-tumor efficiency.[166] In another study, a core–shell porphyrin-MOF was created, which, when exposed to a NIR laser, was operated as a potential cascade biocatalyst for the breakdown of glucose into H_2O_2 and H_2O_2 into O_2, resulting in the continuous production of $^1O_2$.[167]

As noted, type II photodynamic therapy is the most prevalent type. This is because type I mechanism investigation is still very challenging in PDT because of the restricted electron transition from PS to GS oxygen, which forms the $O_2^{\bullet -}$. Nonetheless, a recent recommendation addresses this problem in some way. Due to the polarized COFs with aggravated local polarization, a novel type I PDT route was effectively created. The process is followed by the chemical adsorption of oxygen, which is subsequently reduced to $O_2^{\bullet -}$ by photo-induced electrons and oxidized to $^1O_2$ by holes. Further suppression of recombining electron–hole and increased light absorption following the protonation of the COF's imine bond encouraged the production of ROS.[168]

Additional tactics are also suggested to improve PDT's efficacy. It is demonstrated that the imidazole-linked porphyrin-containing COF can effectively start the production of $^1O_2$ when exposed to visible light. This efficiency exceeds that of the pristine porphyrin-containing reactant and even surpasses some widely utilized, commercially accessible photosensitizing species, as demonstrated in Fig. 6(b).[159] Complete tumor elimination is challenging to accomplish with PDT or PTT alone.

Tumor hypoxia limits PDT, while PTT makes tumor cells thermoresistant. Even yet, PTT can enhance PDT's benefits by boosting blood flow to improve the oxygen delivered to tumor tissues, and PDT also gets rid of PTT's heat-resistant cancer cells. As a result, PDT and PTT working together can have synergistic impacts for extremely successful tumor removal. A documented case in point is the carboxylated porphyrin MOF with defect engineering, which combines the multimodal properties of two phototherapeutic agents to produce multiple imaging-guided synergistic PDT/PTT and multiple diagnostic imaging, thereby considerably improving cancer therapy.[133] The problem of insufficient phototherapy alone can be resolved by combining phototherapy with other forms of treatment. The potential synergistic effect of combining several therapy options warrants more investigation, as opposed to merely combining disparate therapeutic modalities.[61] Due to these valuable compounds' proven ability to act as efficient drug carriers, by adding anti-cancer drugs, the goal of enhancing phototherapy efficiency will be achieved (Fig. 6(c)).[160]

Compared to standard monotherapy, PMOFs loaded with targeted compounds can quickly reach the tumor site and accumulate a significant amount.[71] MOFs are distinguished from other drug delivery systems because of their superior stability, facile ROS diffusion out of the framework, and increased PS loading capacity.[160] Sequential synergistic therapy has received much attention lately.[169] The use of PMOFs in PDT-assisted cancer treatment is not restricted to certain types of cancer. For example, a precise synergy between PDT and autophagy inhibition was achieved by combining the bionic functionalized surface's immune-escape and homologous targeting tendencies with PDT. Thus, the field of non-invasive oropharyngeal carcinoma detection and therapy was broadened by the highly effective

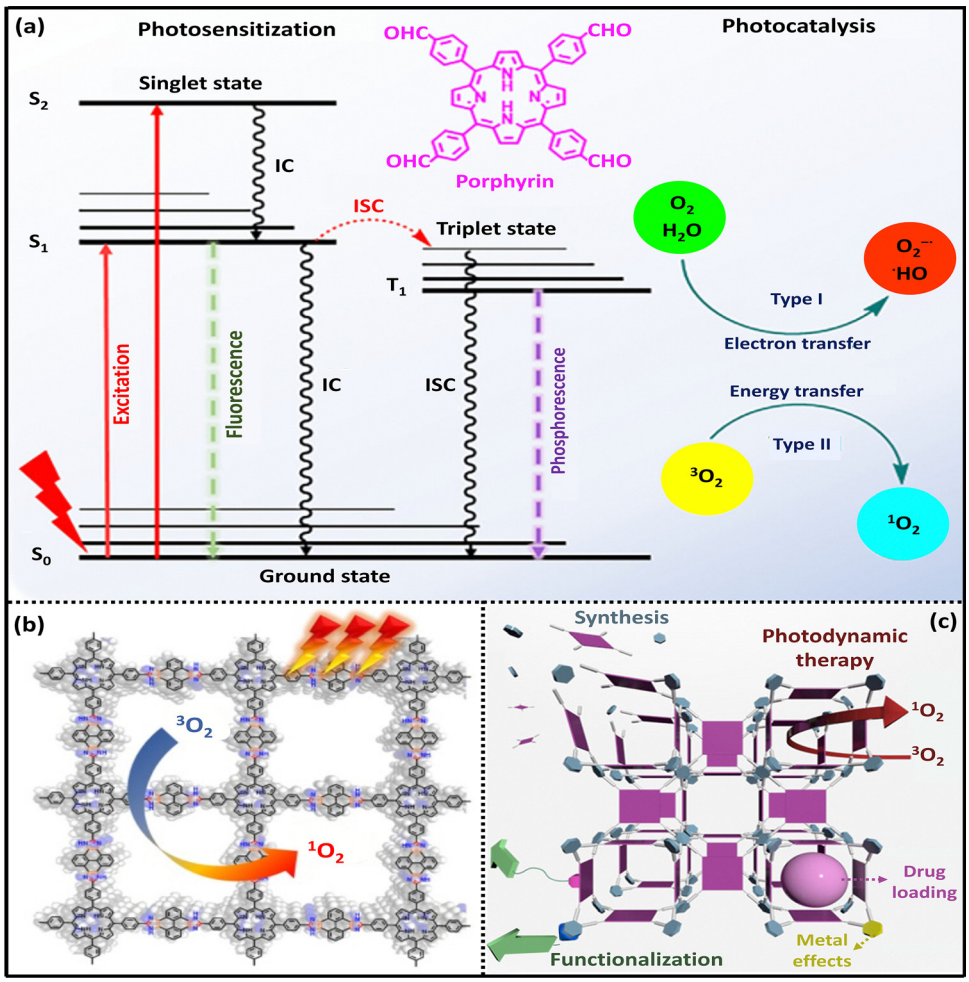

Fig. 6 (a) Porphyrin-based PDT schematic to illustrate each level's visual explanation and order. This figure was reproduced from *Aggregate*, 2024, **5**, 1–18.[80] (b) An example of an imidazole-linked porphyrin-COF producing $^1O_2$ in the presence of light. This figure was reproduced from *ACS Nano*, 2022, **16**, 21565–21575.[159] (c) PS-based MOFs from fundamental chemistry to the structural connection with biological use in PDT. This figure was reproduced from *Mater. Sci. Eng., C*, 2021, **131**, 112514.[160]

impact on tumor suppression.[170] When utilized in PDT, Zn-MOFs' large specific surface area, changeable porosity, and modifiable sites can provide exceptional benefits. ZIFs are a subclass of MOFs that have outstanding thermal, hydrothermal, and stability characteristics.[171] The most popular among researchers was ZIF-8, particularly when changed by TCPP.[172] ZIF-8 NPs, the most traditional and widely used ZIF for cancer treatment, are composed of 2-methylimidazole and zinc.[173] ZIF-8's targeted drug delivery causes it to highly aggregate at the tumor location, minimizing harm to healthy tissue. Utilized in drug delivery, synergistic PDT, drug-loaded Zn-MOFs can release Zn^{2+} under acidic conditions. Drug-loaded Zn-MOFs exhibit an enhanced PDT effect and increased ROS generation due to the release of coordination bonds and specific catalytic actions.[172] There have also been reports on ZIF-8 functionalized compounds being used to treat skin-related issues, including skin cancer.[174]

The TCPP with tirapazamine was used to treat breast cancer.[169] Effective DOX loading on biocompatible graphene oxide and MOF-Fe–porphyrin nanoplatforms against 4T1 cancer cells, with good fluorescence imaging and magnetic resonance imaging (MRI) capabilities[175] and improved PDT and DOX drug delivery system using ultra-thin porphyrin-based MOF nanosheets with high drug loading[176] can be mentioned as instances of recent studies on a highly recommended combination of chemotherapy and improved PDT.

It has also been observed that some novel techniques (such as constructing an enzyme nanopocket with a porphyrin COF) have been reported to increase PDT efficacy while simultaneously improving anti-cancer efficacy *via* the synergistic improvement of long-lasting starving treatment.[177] Additionally, metals in the framework enable an effect on PDT attenuators, including tumor hypoxia and intracellular antioxidants, such as glutathione enzyme, thereby providing a more favorable intracellular environment for photodynamic action.[160]

Through increased permeability and retention effects, porphyrin MOF NPs (nMOFs) can accumulate in tumors and produce cytotoxic singlet oxygen, which kills the tumor cells. However, the singlet oxygen generated by the porphyrin MOF can be burst by intracellular glutathione, and tumor cells have a significantly higher intracellular glutathione level than other

normal cells.[178] Additionally, Mn-MOFs provide O_2 on their own while demonstrating catalase-like activity and lowering glutathione levels *in vitro*. A porphyrin–nMOF core and (MnO_2 shell) was created and published in this regard to reduce tumor hypoxia in chemo-photodynamic synergistic therapy.[179,180]

5.2. Photothermal therapy

Numerous photothermal agents have been utilized in cancer therapy to date. Depending on the various components, these materials are either inorganic or organic photothermal materials. Large extinction coefficients, ease of superficial functionalization, effective photothermal conversion, and improved photostability are just a few of the exceptional qualities that inorganic photothermal materials often offer. However, they are also expensive, poorly biodegradable, and poisonous over the long run. Organic photothermal materials are more biodegradable and biocompatible; however, their use in PTT is limited by their challenging synthesis processes, modest photothermal conversion efficacy, and limited photothermal stability. Because single inorganic or organic materials cannot have a suitable therapeutic impact, organic–inorganic composite compounds with increased efficiency for the PTT of cancer are highly desirable.[60] PTT could potentially be built with porphyrins, commonly known as traditional PSs. This was because of their potent π–π stacking interactions in aggregated forms, including porphysomes, which changed the excited energy dissipation procedure from radiative decay and ISC processes to a thermal deactivation procedure that produced heat.[181]

Due to their exceptional heat stability, high specific surface areas, and distinct structural characteristics, MIL-100(Fe) and MIL-101(Fe) have been recognized as promising candidates for PTT therapy of cancers.[182] Through non-radiative vibration relaxation, the excited electron of porphyrinic MOFs exposed to light could revert to the GS for PTT.[80] PMOFs' large pore size and space allow for the effective loading of PTAs for PTT.[71] One practical recent example in this regard is a mixed-porphyrin ligand MOF, where high drug loading efficiency was achieved through the MOF's channel. The composite demonstrated improved PDT and tumor-targeted redox-responsive drug release following superficial modification by hyaluronic acid *via* a disulfide bond. Due to the efficient synergistic chemotherapy, improved PDT, and PTT, the composite clearly reduced tumor growth.[183] Table 3 compiles current examples of COFs and MOFs based on porphyrins. The benefits of combining phototherapy with other therapies are also stated in most cases.

Depending on how PTAs and COFs interact, there are two types of COF-based PTT:

a. COFs, including material composites with photothermal properties.

b. COFs having inherent photothermal characteristics.[79,198]

For example, *in situ*-produced CuS could be utilized concurrently as a photothermal agent for PTT in a Cu(II)–porphyrin-derived nanoscale COF. Notably, improved PDT could result from the controlled release of $^1O_2$.[154]

COFs with distinct electron and hole transport channels enable ROS formation through type-I PDT by inducing exciton dissociation and facilitating charge carrier transport. Moreover, the photoexcited species' geminate and non-geminate recombination results in a non-radiative attenuation route that facilitates photothermal conversion. Therefore, synergistic type-I PDT and PTT are made possible by a suitable equilibrium between these mechanisms.[78]

Since PTT uses laser light to cause hyperthermia, it successfully ablates malignancies. Further harm could unavoidably be caused by the heat spreading to the nearby healthy tissues. Helpful strategies are presented to solve this issue. The minor side effects on healthy tissues are made achievable by the combined impact of gambogic acid, which enhances thermal damage, and porphyrin COFs for photothermal conversion with single laser irradiation.[199]

6. Conclusions and future perspectives

This review highlights the explosive trend in recent years, with porphyrin-comprising MOFs and COFs used in phototherapy. Due to superior photophysical qualities, porphyrins and their derivatives are occasionally employed as PSs for PDT. MOFs are substances with multi-functionality, enhanced porosity, tunable architectures, biocompatibility, and biodegradability. Research has shown that developing porphyrin-containing MOFs could get around the drawbacks of free porphyrins but combine the functions of MOFs and porphyrins and enhance their physicochemical characteristics. To date, porphyrin@MOFs, porphyrinic MOFs, and porphyrinic MOF composites have been synthesized using various techniques. A large number of methodologies have been suggested to enhance the therapeutic efficiency of porphyrin-containing MOFs in PTT and PDT, including heavy-atom replacement of the porphyrinic MOFs, manipulation of particle size, controlled preparation, and functionalization with targeting species or functional groups. Furthermore, the logical construction of functional elements in MOFs enables the disruption of survival processes and modification of the tumor microenvironment to improve phototherapy efficacy. Improving PDT and PTT of tumors is possible by optimizing the fabrication of porphyrin-comprising MOFs.

On the other hand, COFs exhibit a high degree of chemical stability and a well-regulated structure, whereas porphyrins possess long excited-state lifetimes and remarkable light absorption capabilities. Porphyrin-comprising COFs are anticipated to exhibit distinct charge separation or transfer and photo-electric conversion behaviors since porphyrins serve as the functional unit in these systems. Despite the benefits discussed in this paper, phototherapy still has several drawbacks, including oxygen dependence, uneven heat distribution, and restricted tissue penetration, among others. Subsequent studies on phototherapy may be combined with various therapeutic approaches, including radiation therapy, chemotherapy, starvation treatment, gas therapy, and immunotherapy.

The regulatory environment for MOFs and COFs in future clinical applications presents several challenges, particularly in

Table 3 Recent platforms and their effects on developing cancer phototherapy

Entry	Platform	Primary recommended usage	Additional application	Target/cell line/disease	Highlights and outcomes	Ref.
1	Hyaluronic acid@sulfasalazine@FeMOF	PDT	Chemotherapy (sulfasalazine)	—	Reducing endogenous glutathione levels, overcoming apoptosis resistance, and consistently producing ROS all improved PDT efficacy	184
2	(upconversion NPs, $NaYF_4$: 20%Yb,1%Tm@$NaYF_4$:10% Yb@$NaNdF_4$)-ferric zirconium porphyrin MOF	PDT	Sonodynamic therapy/ fluorescence imaging and T_2-weighted MRI	—	For PDTs under 808 nm laser irradiation, the ROS production was encouraged, and oxygen was supplied by Fe^{3+} ions	185
3	Iniparib@MOF-(PCN-224(Mn))-polydopamine-modified hyaluronic acid	PDT	PTT/chemotherapy (iniparib)	—	Biodegradable oxygen-producing nanoplatforms were utilized to enhance PDT and PTT under an 808 nm laser, thereby combating tumor-associated hypoxia	186
4	Zr(IV)-based porphyrinic MOFs@DOX/ZIFs	PDT	Chemotherapy (DOX)	—	Combining pH-controlled drug delivery and effective $^1O_2$ production under light irradiation allowed PDT and chemotherapy to work synergistically	187
5	Au@MOF core–shell hybrids	PDT/PTT	—	—	Au nanorod cores' high absorbance at 650 nm was the primary cause of the PTT effect. Under light circumstances, the porphyrin ligand in the MOF shell could transform O_2 into $^1O_2$, leading to a high PDT effect	188
6	Porphyrinic MOF@CuS	PDT/PTT	Chemodynamic therapy	4T1 cells	The hybrid nanocomposites successfully performed PTT, PDT, and CDT activities and destroyed the cancer cells	189
7	TCPP in PCN-600-DOX@polydopamine	PDT/PTT	Chemotherapy (DOX)	4T1 cells	Excellent biocompatibility and anti-cancer ability were demonstrated in *in vivo* testing by the triple synergistic technique shown	190
8	Liposome-coated core–shell gold nanostars@nanoscale MOF nanocomposite encapsulated with gambogic acid	PDT/PTT	Chemotherapy (gambogic acid)	Breast cancer	In addition to creating a hypoxic environment inside solid tumors and enhancing the PDT effect, heat-resistant tumor cells were destroyed by ROS produced by 660 nm laser radiation	191
9	Porphyrin-based organic polymer coated ZIF-8	PDT/PTT		Lung cancer	Compared to traditional physical adsorption techniques, the described core–shell structure offers tumor-specificity, biocompatibility, low cost, and improved optical property preservation	192
10	Fluoropyrimidine 5-fluorouracil-nano disulfide-linked porphyrin-COF	PDT	Chemotherapy (fluoropyrimidine 5-fluorouracil)	MCF-7 breast cancer	Improved PDT in conjunction with selective medication release is achieved.	193
11	DOX@porphyrin-COF@hyaluronic acid	PDT	Chemotherapy (DOX)	4T1 cells	Combined application of photodynamic therapy with drug aggregation and targeted release in chemotherapy was successful	194
12	ICG@porphyrin-based COF NPs	PTT	Chemotherapy (ICG)	4T1 tumor-bearing mice	Strong photothermal effects were obtained upon exposure to laser radiation, resulting in the elimination of tumor cells	195
13	Gambogic acid@porphyrinic COF@ dopamine hydrochloride	PTT	PDT/chemotherapy	4T1 cells	The tumor cells' resistance to heat was reversed, and phototherapy was improved. It has been applied to prevent the primary and spread of tumors at low temperatures	196
14	Porphyrin based-COF	PDT/PTT	—	H22 tumor-bearing mice	The remarkable anti-cancer performance was achieved due to the photothermal impact and extraordinarily high intratumoral ROS level of the produced NPs	197

terms of toxicity analysis and large-scale synthesis. First and foremost, a crucial regulatory obstacle is the thorough evaluation of toxicity and biocompatibility. The toxicity of MOFs is primarily determined by their unique chemistry, particle size, shape, and aggregation state, due to their extreme variety resulting from almost unlimited combinations of metal ions and organic linkers. For instance, research studies suggest that MOFs with copper (Cu) and manganese (Mn) are often very hazardous. Still, those with zinc (Zn), iron (Fe), cobalt (Co), and aluminum (Al) are moderately toxic, and those with chromium (Cr), zirconium (Zr), and magnesium (Mg) are typically low-harmful. The generation of ROS and the discharge of hazardous mechanisms of MOF toxicity can result in genotoxicity, inflammation, and cellular damage. The size of nMOFs is also an important consideration. Although nMOFs are typically more biocompatible than micron-sized MOFs, toxicity can rise sharply when particle size drops below around 200 nm because of increased cellular penetration and reactivity. The lack of defined exposure limits and consistent toxicity testing procedures remains a significant obstacle, despite many encouraging findings. Since MOF decomposition and the ensuing release of metal ions may cause toxicity and inflammation, long-term *in vivo* biocompatibility and stability assessments are also essential. To prevent the synthesis of hazardous compounds for use in biomedicine, a deeper understanding of the relationship between MOF structure factors and their toxicity is required. In the second place, MOFs/COFs have significant practical regulatory obstacles when synthesized on a wide scale. To ensure cost-effectiveness, safety, and repeatability, several key factors must be carefully considered when transitioning from laboratory-scale to industrial-scale production. Several solutions exist to overcome these hurdles, including the selection of raw materials, the choice of synthesis methods, and the control and optimization of post-synthesis processing, all of which require close collaboration between academia and industry.[200–204]

An additional concern is that phototherapy has significant limitations due to restricted penetration. Deeply seated cancers and infections remain challenging to treat with phototherapy, even though the therapeutic depth can be increased by utilizing upconversion NPs and two-photon-activated PSs. Another crucial auxiliary technique in phototherapy is imaging guidance, which can be used to locate and characterize lesions, as well as track the distribution of therapeutic chemicals to deliver the right amount of irradiation. More significantly, implanting a light source is preferable in solid organs under the supervision of fluorescence, allowing for the treatment of deep lesions. MOFs are desired carriers for such functionalities, considering these issues. Thus far, combination therapy and imaging-assisted therapy, aided by MOFs, have shown favorable results. However, precise control, high efficacy, prevention of resistance development, and reduced tissue damage remain under research before being implemented in a clinical setting.

Furthermore, combining PDT and PTT in porphyrin-comprising COFs could boost their anti-tumor effects. Porphyrin-comprising COF NPs may produce ROS and heat when exposed to a single wavelength of light. Thus, this could be employed as a reagent with photoactivity to combine PDT and PTT *in vivo*. Porphyrin-comprising COFs' anti-degradation capacity improves their biosafety and allows precision anti-tumor treatment *in vivo* using photoacoustic imaging. Porphyrin-comprising COFs have an ordered conjugated structure that boosts light absorption, minimizes carrier recombination, and improves phototherapy efficiency.

Several studies have focused on enhancing the efficacy of PSs and PTAs in terms of their ROS yield and photothermal transformation. However, other physicochemical characteristics of materials, such as crystallinity, aqueous stability, and degradability, must also be taken into account. To design MOFs with preferred ROS yields, photothermal transformation efficacy, and additional photo-related functionalities in the future, it will be necessary to clarify the specific photodynamic and photothermal mechanisms. Integrated therapy, on the other hand, involves the use of various therapeutic agents with diverse roles. Further studies should be conducted to investigate the therapeutic mechanisms by which these medicines exhibit synergy. In other areas, a complete correlation among structure, characteristics, composition, and efficiency can be formulated, including the marking of MOF shape and crystalline structure, core–shell interface interactions, drug synergy with ROS, and so on, if the respective mechanisms are thoroughly understood. This correlation is beneficial for producing highly effective medicinal materials as opposed to the ones that are only structurally complex.

While the majority of published MOF-based PSs or PTAs target cancer therapy, several other disciplines are also showing promise due to the production of ROS and temperature increases induced by light exposure. Moreover, PTAs and red cell membranes have been fused to form an anticorrosive coating for magnesium alloy implants that can self-repair upon exposure to light of a specific wavelength.[205] Numerous fields with different requirements for temperature increments, generation of ROS, and light penetration can thus be viewed as candidates for further applications of PDT and PTT. In addition to conventional methods of material manufacturing, like encapsulation and surface coating, biomineralization, which blends materials with bacteria and viruses, is also used for phototherapy.[206,207]

In summary, COFs and MOFs in phototherapy have advanced significantly over the past few decades. With their numerous combined roles, MOFs can enhance the effectiveness of conventional phototherapy under logical design, a development that is gaining increasing attention. The study on MOFs in phototherapy is still in its early stages despite recent publications showing their sophisticated design and high therapeutic performance. They must, however, undergo a tremendous amount of work before they can be considered for clinical trial testing. Due to their specialized photo-electric and photothermal characteristics, porphyrin-comprising COFs exhibit great promise in the biomedical industry and are a strong way to address the field's problems. Nevertheless, most COFs encounter challenges, such as difficult preparation methods and long-term biocompatibility issues, which somewhat restrict their practical use. As a result, COFs and MOFs used in phototherapy will continue to grow and play a significant role in medical care.

Author contributions

Fatemeh Ganjali: conceptualization, writing – review and editing; Saminalsadat Sehat: investigation, writing – original draft, writing – review and editing; Sepide Azadegan: investigation, writing – original draft, writing – review and editing; Maryam Saidi Mehrabad: investigation, writing – review and editing; Leila Choopani: investigation, visualization; Ali Maleki: conceptualization, supervision, project administration, validation, writing – original draft, writing – review and editing.

Conflicts of interest

The authors declare that they have no known competing financial interests or personal relationships that could have appeared to influence the work reported in this paper.

Data availability

No primary research results, software or code have been included and no new data were generated or analysed as part of this review.

Acknowledgements

The authors gratefully acknowledge the partial support from the Research Council of the Iran University of Science and Technology (IUST).

References

1 D. T. Debela, S. G. Muzazu, K. D. Heraro, M. T. Ndalama, B. W. Mesele, D. C. Haile, S. K. Kitui and T. Manyazewal, *SAGE Open Med.*, 2021, **9**, 20503121211034366.
2 M. Cagel, E. Grotz, E. Bernabeu, M. A. Moretton and D. A. Chiappetta, *Drug Discovery Today*, 2017, **22**, 270–281.
3 J. Sharifi-Rad, C. Quispe, J. K. Patra, Y. D. Singh, M. K. Panda, G. Das, C. O. Adetunji, O. S. Michael, O. Sytar and L. Polito, *Oxid. Med. Cell. Longevity*, 2021, **2021**, 3687700.
4 J. Chen, Z. Zhang, J. Ma, A. Nezamzadeh-Ejhieh, C. Lu, Y. Pan, J. Liu and Z. Bai, *Dalton Trans.*, 2023, **52**, 6226–6238.
5 Z. Xie, T. Fan, J. An, W. Choi, Y. Duo, Y. Ge, B. Zhang, G. Nie, N. Xie and T. Zheng, *Chem. Soc. Rev.*, 2020, **49**, 8065–8087.
6 B. Zhang, S. Yu, L. Zhou, J. Feng, D. Xie and G. Ma, *Colloids Surf., A*, 2023, **673**, 131805.
7 Z. Zhou, Y. Sun, J. Shen, J. Wei, C. Yu, B. Kong, W. Liu, H. Yang, S. Yang and W. Wang, *Biomater.*, 2014, **35**, 7470–7478.
8 S. Chen, F. Tang, L. Tang and L. Li, *ACS Appl. Mater. Interfaces*, 2017, **9**, 20895–20903.
9 L.-C. Cheng, J.-H. Huang, H. M. Chen, T.-C. Lai, K.-Y. Yang, R.-S. Liu, M. Hsiao, C.-H. Chen, L.-J. Her and D. P. Tsai, *J. Mater. Chem.*, 2012, **22**, 2244–2253.
10 H. Chen, P. Timashev, Y. Zhang, X. Xue and X.-J. Liang, *RSC Adv.*, 2022, **12**, 9725–9737.
11 X. Xue, A. Lindstrom and Y. Li, *Bioconjugate Chem.*, 2019, **30**, 1585–1603.
12 Z. Liu, H. Li, Z. Tian, X. Liu, Y. Guo, J. He, Z. Wang, T. Zhou and Y. Liu, *ChemPlusChem*, 2022, **87**, e202200156.
13 K. Bera, S. Maiti, M. Maity, C. Mandal and N. C. Maiti, *ACS Omega*, 2018, **3**, 4602–4619.
14 X. Wang, F. Yan, X. Liu, P. Wang, S. Shao, Y. Sun, Z. Sheng, Q. Liu, J. F. Lovell and H. Zheng, *J. Controlled Release*, 2018, **286**, 358–368.
15 R. Sheikhsamany and A. Nezamzadeh-Ejhieh, *J. Mol. Liq.*, 2024, **414**, 126265.
16 Y. Zou, J. Chen, X. Luo, Y. Qu, M. Zhou, R. Xia, W. Wang and X. Zheng, *Front. Pharmacol.*, 2024, **15**, 1481168.
17 X. Chen, R. Tong, Z. Shi, B. Yang, H. Liu, S. Ding, X. Wang, Q. Lei, J. Wu and W. Fang, *ACS Appl. Mater. Interfaces*, 2018, **10**, 2328–2337.
18 M. C. Scicluna and L. Vella-Zarb, *ACS Appl. Nano Mater.*, 2020, **3**, 3097–3115.
19 T. Sun, R. Xia, J. Zhou, X. Zheng, S. Liu and Z. Xie, *Mater. Chem. Front.*, 2020, **4**, 2346–2356.
20 Q. Zheng, X. Liu, Y. Zheng, K. W. Yeung, Z. Cui, Y. Liang, Z. Li, S. Zhu, X. Wang and S. Wu, *Chem. Soc. Rev.*, 2021, **50**, 5086–5125.
21 D. K. Gupta, S. Kumar and M. Y. Wani, *J. Mater. Chem. B*, 2024, **12**, 2691–2710.
22 P. Gao, M. Wang, Y. Chen, W. Pan, P. Zhou, X. Wan, N. Li and B. Tang, *Chem. Sci.*, 2020, **11**, 6882–6888.
23 Z. Luo, Y. Sheng, C. Jiang, Y. Pan, X. Wang, A. Nezamzadeh-Ejhieh, J. Ouyang, C. Lu and J. Liu, *Dalton Trans.*, 2023, **52**, 17601–17622.
24 K. Zhang, X. Meng, Y. Cao, Z. Yang, H. Dong, Y. Zhang, H. Lu, Z. Shi and X. Zhang, *Adv. Funct. Mater.*, 2018, **28**, 1804634.
25 J. Chen, Y. Zhu and S. Kaskel, *Angew. Chem., Int. Ed.*, 2021, **60**, 5010–5035.
26 O. M. Yaghi, G. Li and H. Li, *Nature*, 1995, **378**, 703–706.
27 O. M. Yaghi and H. Li, *J. Am. Chem. Soc.*, 1995, **117**, 10401–10402.
28 B. F. Abrahams, B. F. Hoskins and R. Robson, *J. Am. Chem. Soc.*, 1991, **113**, 3606–3607.
29 G. Lin, H. Ding, R. Chen, Z. Peng, B. Wang and C. Wang, *J. Am. Chem. Soc.*, 2017, **139**, 8705–8709.
30 S. Gan, X. Tong, Y. Zhang, J. Wu, Y. Hu and A. Yuan, *Adv. Funct. Mater.*, 2019, **29**, 1902757.
31 A. P. Cote, A. I. Benin, N. W. Ockwig, M. O'Keeffe, A. J. Matzger and O. M. Yaghi, *Science*, 2005, **310**, 1166–1170.
32 J. Hu, J. Hu, W. Wu, Y. Qin, J. Fu, C. Liu, P. H. Seeberger and J. Yin, *Acta Biomater.*, 2022, **148**, 206–217.
33 X.-H. Liu, J.-Y. Yue, Y.-P. Mo, Y. Yao, C. Zeng, T. Chen, H.-J. Yan, Z.-H. Wang, D. Wang and L.-J. Wan, *J. Phys. Chem. C*, 2016, **120**, 15753–15757.
34 H. Wang, Y. Chen, H. Wang, X. Liu, X. Zhou and F. Wang, *Angew. Chem., Int. Ed.*, 2019, **131**, 7458–7462.
35 P. Ghorbani, A. Abbasi and S. Zamani, *J. Phys. Chem. Solids*, 2024, 112271.
36 Y. Lin, T. Zhou, R. Bai and Y. Xie, *J. Enzyme Inhib. Med. Chem.*, 2020, **35**, 1080–1099.
37 J. Jiao, J. He, M. Li, J. Yang, H. Yang, X. Wang and S. Yang, *Nanoscale*, 2022, **14**, 6373–6383.

38 X. Liang, M. Chen, P. Bhattarai, S. Hameed, Y. Tang and Z. Dai, *ACS Nano*, 2021, **15**, 20164–20180.
39 T. J. Dougherty, J. E. Kaufman, A. Goldfarb, K. R. Weishaupt, D. Boyle and A. Mittleman, *Cancer Res.*, 1978, **38**, 2628–2635.
40 Z. Tian, H. Li, Z. Liu, L. Yang, C. Zhang, J. He, W. Ai and Y. Liu, *Curr. Treat. Options Oncol.*, 2023, **24**, 1274–1292.
41 S. Bouramtane, L. Bretin, A. Pinon, D. Leger, B. Liagre, L. Richard, F. Brégier, V. Sol and V. Chaleix, *Carbohydr. Polym.*, 2019, **213**, 168–175.
42 M. Li, Y. Xu, Z. Pu, T. Xiong, H. Huang, S. Long, S. Son, L. Yu, N. Singh and Y. Tong, *Proc. Natl. Acad. Sci. U. S. A.*, 2022, **119**, e2210504119.
43 H. Montaseri, C. A. Kruger and H. Abrahamse, *Int. J. Mol. Sci.*, 2020, **21**, 3358.
44 M. Akbari Oryani, M. Tarin, L. Rahnama Araghi, F. Rastin, H. Javid, A. Hashemzadeh and M. Karimi-Shahri, *J. Drug Targeting*, 2025, **33**, 473–491.
45 X. Zheng, Q. Zhang, X. Wang, J. Chen, J. Wu, M. Zhou, R. Xia, W. Wang and Z. Xie, *Chem. Commun.*, 2024, **60**, 13641–13652.
46 C. Qi, J. Chen, Y. Qu, X. Luo, W. Wang and X. Zheng, *Pharmaceutics*, 2024, **16**, 1625.
47 J.-J. Qian, J.-X. Guo, M.-C. Wang, L.-J. Chen, X. Zhao and X.-P. Yan, *J. Colloid Interface Sci.*, 2025, **692**, 137494.
48 S. Shyam Sunder, U. C. Sharma and S. Pokharel, *Signal Transduction Targeted Ther.*, 2023, **8**, 262.
49 M. Z. Quazi, J. Park and N. Park, *Technol. Cancer Res. Treat.*, 2023, **22**, 15330338231170939.
50 N. Rarokar, S. Gurav, D. M. Kokare, V. Kale and N. A. Raut, *Photophysics and Nanophysics in Therapeutics*, 2022, pp. 3–14.
51 X. Li, C. Tang, L. Zhang, M. Song, Y. Zhang and S. Wang, *Biomimetics*, 2023, **8**, 171.
52 M. Xia, Y. Yan, H. Pu, X. Du, J. Liang, Y. Sun, J. Zheng and Y. Yuan, *Chem. Eng. J.*, 2022, **442**, 136295.
53 H. Li, W. Xiao, Z. Tian, Z. Liu, L. Shi, Y. Wang, Y. Liu and Y. Liu, *Photodiagn. Photodyn. Ther.*, 2023, **41**, 103236.
54 S. Ghattavi and A. Nezamzadeh-Ejhieh, *Composites, Part B*, 2020, **183**, 107712.
55 W. Yu, W. Zhen, Q. Zhang, Y. Li, H. Luo, J. He and Y. Liu, *ChemMedChem*, 2020, **15**, 1766–1775.
56 A. Pinto and M. Pocard, *Pleura Peritoneum*, 2018, **3**, 20180124.
57 K. Guidolin, L. Ding, J. Chen, B. C. Wilson and G. Zheng, *Nanophotonics*, 2021, **10**, 3161–3168.
58 J. Yang, D. Dai, X. Zhang, L. Teng, L. Ma and Y.-W. Yang, *Theranostics*, 2023, **13**, 295.
59 L. Huang, S. Zhao, J. Wu, L. Yu, N. Singh, K. Yang, M. Lan, P. Wang and J. S. Kim, *Coord. Chem. Rev.*, 2021, **438**, 213888.
60 J. Li, W. Zhang, W. Ji, J. Wang, N. Wang, W. Wu, Q. Wu, X. Hou, W. Hu and L. Li, *J. Mater. Chem. B*, 2021, **9**, 7909–7926.
61 X. Deng, Z. Shao and Y. Zhao, *Adv. Sci.*, 2021, **8**, 2002504.
62 J. Tian, B. Huang, M. H. Nawaz and W. Zhang, *Coord. Chem. Rev.*, 2020, **420**, 213410.
63 M. Falsafi, M. Zahiri, A. S. Saljooghi, K. Abnous, S. M. Taghdisi, A. Sazgarnia, M. Ramezani and M. Alibolandi, *Microporous Mesoporous Mater.*, 2021, **325**, 111337.
64 N. Plekhova, O. Shevchenko, O. Korshunova, A. Stepanyugina, I. Tananaev and V. Apanasevich, *Bioengineering*, 2022, **9**, 82.
65 H. Duan, F. Wang, W. Xu, G. Sheng, Z. Sun and H. Chu, *Dalton Trans.*, 2023, **52**, 16085–16102.
66 H. Yang, D. Liao, Z. Cai, Y. Zhang, A. Nezamzadeh-Ejhieh, M. Zheng, J. Liu, Z. Bai and H. Song, *RSC Med. Chem.*, 2023, **14**, 2473–2495.
67 J. Yu, W. Chen, L. Qin, A. Nezamzadeh-Ejhieh, F. Cheng, W. Liu, J. Liu and Z. Bai, *J. Mol. Struct.*, 2025, **1321**, 139984.
68 J. Chen, F. Cheng, D. Luo, J. Huang, J. Ouyang, A. Nezamzadeh-Ejhieh, M. S. Khan, J. Liu and Y. Peng, *Dalton Trans.*, 2022, **51**, 14817–14832.
69 Z. Jia, Y. Gao, J. Ni, X. Wu, Z. Mao, G. Sheng and Y. Zhu, *J. Colloid Interface Sci.*, 2023, **629**, 379–390.
70 D. Xu, Q. Duan, H. Yu and W. Dong, *J. Mater. Chem. B*, 2023, **11**, 5976–5989.
71 X. Jiang, Y. Zhao, S. Sun, Y. Xiang, J. Yan, J. Wang and R. Pei, *J. Mater. Chem. B*, 2023, **11**, 6172–6200.
72 X. Liang, M. Mu, B. Chen, R. Fan, H. Chen, B. Zou, B. Han and G. Guo, *Biomater. Res.*, 2023, **27**, 120.
73 D. Liao, J. Huang, C. Jiang, L. Zhou, M. Zheng, A. Nezamzadeh-Ejhieh, N. Qi, C. Lu and J. Liu, *Pharmaceutics*, 2023, **15**, 2071.
74 Y. Xie, M. Wang, Q. Sun, D. Wang and C. Li, *Adv. Nano-Biomed Res.*, 2023, **3**, 2200136.
75 Q.-X. Wang, Y.-F. Yang, X.-F. Yang, Y. Pan, L.-D. Sun, W.-Y. Zhang, Y. Shao, J. Shen, J. Lin and L. Li, *Nano Today*, 2022, **43**, 101439.
76 Z. Wang, Z. Chen, Z. Zhang, J. Li, K. Chen, H. Liang, L. Lv, Y. Chang, S. Liu and W. Yang, *Nano Today*, 2022, **45**, 101558.
77 S. Yao, Z. Wang and L. Li, *Smart Mater. Med.*, 2022, **3**, 230–242.
78 L. L. Zhou, Q. Guan and Y. B. Dong, *Angew. Chem., Int. Ed.*, 2024, **63**, e202314763.
79 M. Moharramnejad, R. E. Malekshah, Z. Salariyeh, H. Saremi, M. Shahi and A. Ehsani, *Inorg. Chem. Commun.*, 2023, **153**, 110888.
80 Y. Gao, Y. Li, Z. Xu, S. Yu, J. Liu and H. Sun, *Aggregate*, 2024, **5**, e420.
81 Y. Chen, W. Lu, M. Schröder and S. Yang, *Acc. Chem. Res.*, 2023, **56**, 2569–2581.
82 P. Ghorbani, A. Abbasi, S. Zamani and M.-S. Hosseini, *Colloids Surf., A*, 2024, **685**, 133123.
83 H. Mieno, R. Kabe, N. Notsuka, M. D. Allendorf and C. Adachi, *Adv. Opt. Mater.*, 2016, **4**, 1015–1021.
84 W. Zhu, Z.-D. Ding, X. Wang, T. Li, R. Shen, Y. Li, Z. Li, X. Ren and Z.-G. Gu, *Polym. Chem.*, 2017, **8**, 4327–4331.
85 D. Masih, V. Chernikova, O. Shekhah, M. Eddaoudi and O. F. Mohammed, *ACS Appl. Mater. Interfaces*, 2018, **10**, 11399–11405.
86 P. Ling, J. Lei, L. Zhang and H. Ju, *Anal. Chem.*, 2015, **87**, 3957–3963.
87 L. Chen, W. Wang, J. Tian, F. Bu, T. Zhao, M. Liu, R. Lin, F. Zhang, M. Lee and D. Zhao, *Nat. Commun.*, 2021, **12**, 4556.
88 L. G. Ding, S. Wang, B. J. Yao, F. Li, Y. A. Li, G. Y. Zhao and Y. B. Dong, *Adv. Healthcare Mater.*, 2021, **10**, 2001821.

89 C. W. Shields IV, L. L. W. Wang, M. A. Evans and S. Mitragotri, *Adv. Mater.*, 2020, **32**, 1901633.
90 M. Zhang, W. Shen, Q. Jiang, Q. Sun, Y. Liu, Y. Yang and D. Yin, *Colloids Surf., B*, 2022, **214**, 112456.
91 X. Sun, G. He, C. Xiong, C. Wang, X. Lian, L. Hu, Z. Li, S. J. Dalgarno, Y.-W. Yang and J. Tian, *ACS Appl. Mater. Interfaces*, 2021, **13**, 3679–3693.
92 Z. Zhao, Y. Wu, X. Liang, J. Liu, Y. Luo, Y. Zhang, T. Li, C. Liu, X. Luo and J. Chen, *Adv. Sci.*, 2023, **10**, 2303872.
93 H. R. Alanagh, I. Rostami, M. Taleb, X. Gao, Y. Zhang, A. M. Khattak, X. He, L. Li and Z. Tang, *J. Mater. Chem. B*, 2020, **8**, 7899–7903.
94 L. Zhang, L.-L. Yang, S.-C. Wan, Q.-C. Yang, Y. Xiao, H. Deng and Z.-J. Sun, *Nano Lett.*, 2021, **21**, 7979–7988.
95 L. Zhang, Y. Xiao, Q. C. Yang, L. L. Yang, S. C. Wan, S. Wang, L. Zhang, H. Deng and Z. J. Sun, *Adv. Funct. Mater.*, 2022, **32**, 2201542.
96 S. Zamani, A. Abbasi, M. Masteri-Farahani and S. Rayati, *New J. Chem.*, 2022, **46**, 654–662.
97 J. Yang and Y. W. Yang, *Small*, 2020, **16**, 1906846.
98 A. N. Amenaghawon, C. L. Anyalewechi, O. U. Osazuwa, E. A. Elimian, S. O. Eshiemogie, P. K. Oyefolu and H. S. Kusuma, *Sep. Purif. Technol.*, 2023, **311**, 123246.
99 R. Sheikhsamany, A. Nezamzadeh-Ejhieh and R. S. Varma, *Surf. Interfaces*, 2024, **54**, 105205.
100 L. Wang, X. Qu, Y. Zhao, Y. Weng, G. I. Waterhouse, H. Yan, S. Guan and S. Zhou, *ACS Appl. Mater. Interfaces*, 2019, **11**, 35228–35237.
101 Y. Ma, X. Li, A. Li, P. Yang, C. Zhang and B. Tang, *Angew. Chem., Int. Ed.*, 2017, **56**, 13752–13756.
102 S. H. Ghoochani, H. A. Hosseini, Z. Sabouri, M. H. Soheilifar, H. K. Neghab, A. Hashemzadeh, M. Velayati and M. Darroudi, *Lasers Med. Sci.*, 2023, **38**, 151.
103 C. Chen, X. Feng, Q. Zhu, R. Dong, R. Yang, Y. Cheng and C. He, *Inorg. Chem.*, 2019, **58**, 2717–2728.
104 Z. Wang, Q. Sun, B. Liu, Y. Kuang, A. Gulzar, F. He, S. Gai, P. Yang and J. Lin, *Coord. Chem. Rev.*, 2021, **439**, 213945.
105 J. Beamish-Cook, K. Shankland, C. A. Murray and P. Vaqueiro, *Cryst. Growth Des.*, 2021, **21**, 3047–3055.
106 M. Liu, N. Cai, V. Chan and F. Yu, *Nanomaterials*, 2019, **9**, 1306.
107 M.-L. Hu, M. Y. Masoomi and A. Morsali, *Coord. Chem. Rev.*, 2019, **387**, 415–435.
108 S. P. Songca, *J. Photochem. Photobiol.*, 2024, 100245.
109 S. Dutt, A. Kumar and S. Singh, *Clean Technol.*, 2023, **5**, 140–166.
110 L. He, M. Brasino, C. Mao, S. Cho, W. Park, A. P. Goodwin and J. N. Cha, *Small*, 2017, **13**, 1700504.
111 Z. Gharehdaghi, R. Rahimi, S. M. Naghib and F. Molaabasi, *J. Biol. Inorg. Chem.*, 2021, **26**, 689–704.
112 S. M. Sajjadinezhad, L. Boivin, K. Bouarab and P. D. Harvey, *Coord. Chem. Rev.*, 2024, **510**, 215794.
113 L. Feng, Y. Wang, S. Yuan, K.-Y. Wang, J.-L. Li, G. S. Day, D. Qiu, L. Cheng, W.-M. Chen and S. T. Madrahimov, *ACS Catal.*, 2019, **9**, 5111–5118.
114 Q. Zhang, G. Kuang, H. Wang, Y. Zhao, J. Wei and L. Shang, *Adv. Sci.*, 2023, **10**, 2303818.
115 J. Liu, Y. Yang, W. Zhu, X. Yi, Z. Dong, X. Xu, M. Chen, K. Yang, G. Lu and L. Jiang, *Biomaterials*, 2016, **97**, 1–9.
116 J. Yu, Q. Li, Z. Wei, G. Fan, F. Wan and L. Tian, *Acta Biomater.*, 2023, **170**, 330–343.
117 C. Tao, N. Yu, Q. Ren, M. Wen, P. Qiu, S. Niu, M. Li and Z. Chen, *Acta Biomater.*, 2024, **177**, 444–455.
118 L. Zhang, J. Lei, F. Ma, P. Ling, J. Liu and H. Ju, *Chem. Commun.*, 2015, **51**, 10831–10834.
119 Y. Shao, B. Liu, Z. Di, G. Zhang, L.-D. Sun, L. Li and C.-H. Yan, *J. Am. Chem. Soc.*, 2020, **142**, 3939–3946.
120 J. Park, Q. Jiang, D. Feng, L. Mao and H.-C. Zhou, *J. Am. Chem. Soc.*, 2016, **138**, 3518–3525.
121 X. Zheng, L. Wang, Y. Guan, Q. Pei, J. Jiang and Z. Xie, *Biomaterials*, 2020, **235**, 119792.
122 X. Zheng, L. Wang, M. Liu, P. Lei, F. Liu and Z. Xie, *Chem. Mater.*, 2018, **30**, 6867–6876.
123 K. Lu, C. He and W. Lin, *J. Am. Chem. Soc.*, 2014, **136**, 16712–16715.
124 K. Lu, C. He and W. Lin, *J. Am. Chem. Soc.*, 2015, **137**, 7600–7603.
125 X. S. Wang, J. Y. Zeng, M. K. Zhang, X. Zeng and X. Z. Zhang, *Adv. Funct. Mater.*, 2018, **28**, 1801783.
126 Q. Jiang, M. Zhang, Q. Sun, D. Yin, Z. Xuan and Y. Yang, *Mol. Pharm.*, 2021, **18**, 3026–3036.
127 Y. Zhao, J. Wang, X. Cai, P. Ding, H. Lv and R. Pei, *ACS Appl. Mater. Interfaces*, 2020, **12**, 23697–23706.
128 L. Hu, C. Xiong, J.-J. Zou, J. Chen, H. Lin, S. J. Dalgarno, H.-C. Zhou and J. Tian, *ACS Appl. Mater. Interfaces*, 2023, **15**, 25369–25381.
129 Y. Chen, Y. Yang, S. Du, J. Ren, H. Jiang, L. Zhang and J. Zhu, *ACS Appl. Mater. Interfaces*, 2023, **15**, 35884–35894.
130 S.-Y. Li, H. Cheng, B.-R. Xie, W.-X. Qiu, J.-Y. Zeng, C.-X. Li, S.-S. Wan, L. Zhang, W.-L. Liu and X.-Z. Zhang, *ACS Nano*, 2017, **11**, 7006–7018.
131 J.-Y. Zeng, M.-Z. Zou, M. Zhang, X.-S. Wang, X. Zeng, H. Cong and X.-Z. Zhang, *ACS Nano*, 2018, **12**, 4630–4640.
132 H. Wang, D. Yu, J. Fang, C. Cao, Z. Liu, J. Ren and X. Qu, *ACS Nano*, 2019, **13**, 9206–9217.
133 C. Wang, C. Xiong, Z. Li, L. Hu, J. Wei and J. Tian, *Chem. Commun.*, 2021, **57**, 4035–4038.
134 B. Li, X. Wang, L. Chen, Y. Zhou, W. Dang, J. Chang and C. Wu, *Theranostics*, 2018, **8**, 4086.
135 X. Zheng, L. Wang, Q. Pei, S. He, S. Liu and Z. Xie, *Chem. Mater.*, 2017, **29**, 2374–2381.
136 M. Chen, H. Li, C. Liu, J. Liu, Y. Feng, A. G. Wee and B. Zhang, *Coord. Chem. Rev.*, 2021, **435**, 213778.
137 S. Wan, F. Gándara, A. Asano, H. Furukawa, A. Saeki, S. K. Dey, L. Liao, M. W. Ambrogio, Y. Y. Botros and X. Duan, *Chem. Mater.*, 2011, **23**, 4094–4097.
138 D. Wang, Z. Zhang, L. Lin, F. Liu, Y. Wang, Z. Guo, Y. Li, H. Tian and X. Chen, *Biomaterials*, 2019, **223**, 119459.
139 J. Feng, S.-P. Yang, Y.-Q. Shao, Y.-Y. Sun, Z.-L. He, Y. Wang, Y.-N. Zhai and Y.-B. Dong, *Adv. Healthcare Mater.*, 2023, **12**, 2301645.
140 J. Dong, X. Han, Y. Liu, H. Li and Y. Cui, *Angew. Chem., Int. Ed.*, 2020, **59**, 13722–13733.

141 G. Shao, X. Huang, X. Shen, C. Li and A. Thomas, *Adv. Sci.*, 2024, **11**, 2409290.
142 M.-J. Kang, Y.-W. Cho and T.-H. Kim, *Coord. Chem. Rev.*, 2025, **527**, 216400.
143 M. Khulood, U. Jijith, P. Naseef, S. M. Kallungal, V. Geetha and K. Pramod, *Int. J. Pharm.*, 2025, 125380.
144 X.-G. Li, J. Li, J. Chen, L. Rao, L. Zheng, F. Yu, Y. Tang, J. Zheng and J. Ma, *Biomater. Sci.*, 2024, **12**, 2766–2785.
145 F. Liu, I. Rincón, H. G. Baldoví, A. Dhakshinamoorthy, P. Horcajada, S. Rojas, S. Navalón and A. Fateeva, *Inorg. Chem. Front.*, 2024, **11**, 2212–2245.
146 Y. Tai, Z. Chen, T. Luo, B. Luo, C. Deng, Z. Lu, S. Wen and J. Wang, *Adv. Healthcare Mater.*, 2024, **13**, 2303911.
147 Y. Liu, K. Yang, J. Wang, Y. Tian, B. Song and R. Zhang, *Mater. Today Bio*, 2024, **25**, 100981.
148 Y. Zhang, L. Zhang, Z. Wang, F. Wang, L. Kang, F. Cao, K. Dong, J. Ren and X. Qu, *Biomaterials*, 2019, **223**, 119462.
149 S. Liu, Z. Liu, Q. Meng, C. Chen and M. Pang, *ACS Appl. Mater. Interfaces*, 2021, **13**, 56873–56880.
150 Y. Liu, Y. Zhang, X. Li, X. Gao, X. Niu, W. Wang, Q. Wu and Z. Yuan, *Nanoscale*, 2019, **11**, 10429–10438.
151 X. Wan, T. Wu, L. Song, W. Pan, N. Li and B. Tang, *Chem. Commun.*, 2021, **57**, 6145–6148.
152 P. Gao, R. Wei, B. Cui, X. Liu, Y. Chen, W. Pan, N. Li and B. Tang, *Chem. Commun.*, 2021, **57**, 6082–6085.
153 H. He, L. Du, H. Xue, J. Wu and X. Shuai, *Acta Biomater.*, 2022, **149**, 297–306.
154 J. Feng, W.-X. Ren, F. Kong and Y.-B. Dong, *Chem. Commun.*, 2021, **57**, 7240–7243.
155 Y. Shi, S. Liu, Y. Liu, C. Sun, M. Chang, X. Zhao, C. Hu and M. Pang, *ACS Appl. Mater. Interfaces*, 2019, **11**, 12321–12326.
156 C. Valenzuela, C. Chen, M. Sun, Z. Ye and J. Zhang, *J. Mater. Chem. B*, 2021, **9**, 3450–3483.
157 Z. Zhu, Q. Ouyang, L. Zhou, C. Fan, M. Zheng, A. Nezamzadeh-Ejhieh, H. Yuan, Y. Peng and J. Liu, *J. Mol. Struct.*, 2025, **1321**, 139797.
158 Q. Xiang, W. Li, Y. Tan, J. Shi, M. Dong, J. Cheng, J. Huang, W. Zhang, Y. Gong and Q. Yang, *Chem. Eng. J.*, 2022, **444**, 136706.
159 T.-X. Luan, L. Du, J.-R. Wang, K. Li, Q. Zhang, P.-Z. Li and Y. Zhao, *ACS Nano*, 2022, **16**, 21565–21575.
160 S. R. Alves, I. R. Calori and A. C. Tedesco, *Mater. Sci. Eng., C*, 2021, **131**, 112514.
161 J. Ma, Z. Chen, Y. Diao, M. Ye, X. Liu, S. Cui, M. Zhong, A. Nezamzadeh-Ejhieh, J. Liu and J. Ouyang, *React. Funct. Polym.*, 2024, **200**, 105918.
162 Y. Qian, D. Li, Y. Han and H.-L. Jiang, *J. Am. Chem. Soc.*, 2020, **142**, 20763–20771.
163 S. Yang, X. Li, Y. Qin, Y. Cheng, W. Fan, X. Lang, L. Zheng and Q. Cao, *ACS Appl. Mater. Interfaces*, 2021, **13**, 29471–29481.
164 J. Du, T. Shi, S. Long, P. Chen, W. Sun, J. Fan and X. Peng, *Coord. Chem. Rev.*, 2021, **427**, 213604.
165 X. Sun, K. Chen, Y. Liu, G. Zhang, M. Shi, P. Shi and S. Zhang, *Nanoscale Adv.*, 2021, **3**, 6669–6677.
166 G. Gao, Y. Wang, Y. Jiang, S. Luo, M. Li, Y. Cao, Y. Ma and B. Tang, *Inorg. Chem. Front.*, 2024, **11**, 1186–1197.
167 L. He, Q. Ni, J. Mu, W. Fan, L. Liu, Z. Wang, L. Li, W. Tang, Y. Liu and Y. Cheng, *J. Am. Chem. Soc.*, 2020, **142**, 6822–6832.
168 P. Dong, H. Lv, R. Luo, Z. Li, X. Wu and J. Lei, *Chem. Eng. J.*, 2023, **461**, 141817.
169 W.-L. Pan, Y. Tan, W. Meng, N.-H. Huang, Y.-B. Zhao, Z.-Q. Yu, Z. Huang, W.-H. Zhang, B. Sun and J.-X. Chen, *Biomaterials*, 2022, **283**, 121449.
170 M. Guo, Y. Jian, J. Chen, Y. Zhang, A. Nezamzadeh-Ejhieh, X. Deng, Y. Xue, Y. Peng, C. Lu and J. Liu, *Mater. Today Chem.*, 2025, **45**, 102627.
171 J. Li, S. Yin, L. Zhou, A. Nezamzadeh-Ejhieh, Y. Pan, L. Qiu, J. Liu and Z. Zhou, *Biomater. Sci.*, 2024, **12**(23), 5912–5932.
172 M. Li, Z. Zhang, Y. Yu, H. Yuan, A. Nezamzadeh-Ejhieh, J. Liu, Y. Pan and Q. Lan, *Mater. Adv.*, 2023, **4**(21), 5050–5093.
173 Y. Zeng, D. Liao, X. Kong, Q. Huang, M. Zhong, J. Liu, A. Nezamzadeh-Ejhieh, Y. Pan and H. Song, *Colloids Surf., B*, 2023, **232**, 113612.
174 W. Hu, Q. Ouyang, C. Jiang, S. Huang, N.-E. Alireza, D. Guo, J. Liu and Y. Peng, *Mater. Today Chem.*, 2024, **41**, 102300.
175 Z. Fang, E. Yang, Y. Du, D. Gao, G. Wu, Y. Zhang and Y. Shen, *J. Mater. Chem. B*, 2022, **10**, 966–976.
176 R. Zeng, T. He, L. Lu, K. Li, Z. Luo and K. Cai, *J. Mater. Chem. B*, 2021, **9**, 4143–4153.
177 X. Wan, H. Zhang, W. Pan, N. Li and B. Tang, *Chem. Commun.*, 2021, **57**, 5402–5405.
178 Y. Zeng, G. Xu, X. Kong, G. Ye, J. Guo, C. Lu, A. Nezamzadeh-Ejhieh, M. S. Khan, J. Liu and Y. Peng, *Int. J. Pharm.*, 2022, **627**, 122228.
179 Y. Deng, S. Huang, G. Jiang, L. Zhou, A. Nezamzadeh-Ejhieh, J. Liu and Z. Zhou, *RSC Med. Chem.*, 2024, **15**, 2996–3016.
180 D. Zhu, B. Wang, X.-H. Zhu, H.-L. Zhu and S.-Z. Ren, *Nanomedicine*, 2021, **37**, 102440.
181 G. Feng, G.-Q. Zhang and D. Ding, *Chem. Soc. Rev.*, 2020, **49**, 8179–8234.
182 Z. Lin, D. Liao, C. Jiang, A. Nezamzadeh-Ejhieh, M. Zheng, H. Yuan, J. Liu, H. Song and C. Lu, *RSC Med. Chem.*, 2023, **14**, 1914–1933.
183 H. Zhang and X.-B. Yin, *ACS Appl. Mater. Interfaces*, 2022, **14**, 26528–26535.
184 L. Lv, Z. Fu, Q. You, W. Xiao, H. Wang, C. Wang and Y. Yang, *Front. Bioeng. Biotechnol.*, 2024, **11**, 1338257.
185 Z. Wang, B. Liu, Q. Sun, L. Feng, F. He, P. Yang, S. Gai, Z. Quan and J. Lin, *ACS Nano*, 2021, **15**, 12342–12357.
186 L. Feng, M. Chen, R. Li, L. Zhou, C. Wang, P. Ye, X. Hu, J. Yang, Y. Sun and Z. Zhu, *Acta Biomater.*, 2022, **138**, 463–477.
187 B. Liu, Z. Liu, X. Lu, P. Wu, Z. Sun, H. Chu and H. Peng, *Mater. Des.*, 2023, **228**, 111861.
188 X. Cai, Y. Zhao, L. Wang, M. Hu, Z. Wu, L. Liu, W. Zhu and R. Pei, *J. Mater. Chem. B*, 2021, **9**, 6646–6657.
189 G. Wei, X. Lian, X. Qin, Y. Zhao, L. Cai, Q. Chen, J.-J. Zou and J. Tian, *Mater. Des.*, 2022, **224**, 111302.
190 Z. Chen, Y. Sun, J. Wang, X. Zhou, X. Kong, J. Meng and X. Zhang, *ACS Nano*, 2023, **17**, 9003–9013.

191 R.-T. Li, Y.-D. Zhu, W.-Y. Li, Y.-K. Hou, Y.-M. Zou, Y.-H. Zhao, Q. Zou, W.-H. Zhang and J.-X. Chen, *J. Nanobiotechnol.*, 2022, **20**, 212.
192 Y. Tian, Z. Ding, X. Zheng, Y. Li, X. Teng, G. Guo, J. Wang, W. Tan and B. Zhou, *Microporous Mesoporous Mater.*, 2023, **355**, 112562.
193 W.-Y. Li, J.-J. Wan, J.-L. Kan, B. Wang, T. Song, Q. Guan, L.-L. Zhou, Y.-A. Li and Y.-B. Dong, *Chem. Sci.*, 2023, **14**, 1453–1460.
194 P. Chen, Y. Li, Y. Dai, Z. Wang, Y. Zhou, Y. Wang and G. Li, *Photodiagn. Photodyn. Ther.*, 2024, **46**, 104063.
195 S. Tong, C. Li, K. Wang and F. Wu, *Mater. Chem. Front.*, 2024, **8**, 1390–1399.
196 J. Feng, W.-X. Ren, F. Kong, C. Zhang and Y.-B. Dong, *Sci. China Mater.*, 2022, **65**, 1122–1133.
197 D. Dutta, J. Wang, X. Li, Q. Zhou and Z. Ge, *Small*, 2022, **18**, 2202369.
198 Q. Guan, L. L. Zhou, W. Y. Li, Y. A. Li and Y. B. Dong, *Chem. – Eur. J.*, 2020, **26**, 5583–5591.
199 Q. Sun, K. Tang, L. Song, Y. Li, W. Pan, N. Li and B. Tang, *Biomater. Sci.*, 2021, **9**, 7977–7983.
200 D. Chakraborty, A. Yurdusen, G. Mouchaham, F. Nouar and C. Serre, *Adv. Funct. Mater.*, 2024, **34**, 2309089.
201 R. S. Forgan, *Commun. Mater.*, 2024, **5**, 46.
202 Y. Quan, T. F. Parker, Y. Hua, H.-K. Jeong and Q. Wang, *Ind. Eng. Chem. Res.*, 2023, **62**, 5035–5041.
203 P. Wiśniewska, J. Haponiuk, M. R. Saeb, N. Rabiee and S. A. Bencherif, *Chem. Eng. J.*, 2023, **471**, 144400.
204 D. Menon and S. Chakraborty, *Front. Toxicol.*, 2023, **5**, 1233854.
205 L. Huang, J. Li, W. Yuan, X. Liu, Z. Li, Y. Zheng, Y. Liang, S. Zhu, Z. Cui and X. Yang, *Corros. Sci.*, 2020, **163**, 108257.
206 Q. W. Chen, X. H. Liu, J. X. Fan, S. Y. Peng, J. W. Wang, X. N. Wang, C. Zhang, C. J. Liu and X. Z. Zhang, *Adv. Funct. Mater.*, 2020, **30**, 1909806.
207 S. Yan, X. Zeng, Y. Wang and B. F. Liu, *Adv. Healthcare Mater.*, 2020, **9**, 2070036.